




Origin of anastomosis, upper Columbia River, British Columbia, Canada

Eva Lavooi

Student nr.: 3034542
MSc thesis Physical Geography
Faculty of Geosciences, Utrecht University
Final version: 3 October 2010
Supervisors: Dr. M.G. Kleinhans (UU),
Dr. A. Makaske (WUR/Alterra)

Table of contents

List of figures

List of tables

List of appendices

Cover photographs: Own pictures combined with aerial photographs of the upper Columbia River from Patrice Halley.

Preface

This thesis is prepared as a report of my MSc research for the study Physical Geography at the Faculty of Geosciences at Utrecht University. This research consists of fieldwork and analysis of the anastomosing upper Columbia River, southeastern British Columbia, Canada. This research is carried out under supervision of Dr. M.G. Kleinhans (in Utrecht), Dr. A. Makaske (in Utrecht and during the field research) and W. van Dijk (during the field research). Prof. Dr. D.G. Smith was an advisor during the start of the field research. The fieldwork was carried out in cooperation with fellow student Tjalling de Haas.

Funding for the research has been granted by the faculty of Geosciences of Utrecht University, Dr. M.G. Kleinhans and the Molengraaff foundation from the Delft University of Technology.

Acknowledgements

I would like to thank Tjalling de Haas, for the cooperation in the field and clarifying discussions on the theories, calculating the bed load transport rates and reviewing my work. Thanks to Derald Smith for his help in the field and for lending his fieldwork material. Bart Makaske is thanked for his help in the field and his comments on this thesis and help with the drawings of the cross-sections. Thanks to Wim Hoek for all his assistance in the lab by preparing the macrofossils for AMS dating. Also thanks to Hanneke Bos for her help by selecting the macrofossils for the AMS-samples and Gilles Erkens for his view on my theories. I also would like to thank my supervisor, Maarten Kleinhans for his support and useful help and comments. And thanks to Wouter Marra for his mental support and computer technical help during the whole process.

Eva Lavooi

Utrecht, October 2010

Abstract

The upper Columbia River is an anastomosing river. Anastomosing rivers are rivers with multiple, interconnected channels that enclose floodbasins. The origin of anastomosis of the upper Columbia River is a matter of debate. It has been hypothesized that excessive sediment supply causes anastomosis. The aim of this research is to investigate this hypothesis. To do this, the geological and lithological composition of the Columbia Valley fill is investigated. This study brings the results of Makaske et al. (2002, 2009) together with new field data. Two floodplain-wide borehole cross-sections are made during this research, one in an upper highly anastomosing reach and one in a lower weakly anastomosing reach; in order to investigate if the long-term floodplain sedimentation rate in the highly anastomosing reach is higher than in the weakly anastomosing reach. Time control is based on AMS radiocarbon dating of macrofossils, wherefrom sediment budgets are derived. These results are compared with bed load transport predictions made with the present-day river characteristics. The results of these cross-sectional sediment budget analysis pointed out that the deposits in the upper reach consist of more bed-material load than in the lower reach and that the long-term floodplain sedimentation rate in the upper reach is higher than in the lower reach. This is confirmed by the long-term floodplain sedimentation rates calculated with the AMS radiocarbon dates. However, bed load transport predictions show erosion in the upper anastomosing reach and deposition in the lower anastomosing reach. The origin of anastomosis of the upper Columbia River is hence interpreted to be a combination of frequent avulsions and slow abandonment of old channels, whereby avulsions are triggered by excessive sediment supply pulses.

1 Introduction

The upper Columbia River is a well-investigated anastomosing river. Anastomosing rivers are rivers with multiple, interconnected, channels that enclose floodbasins (Makaske, 2001). For a long time they were considered as exceptions rather than common phenomena. In the past three decades, a substantial number of anastomosing river systems has been reported worldwide (Makaske, 1998). But still, the origin of anastomosis is debated in the scientific literature.

1.1 Problem definition and hypothesis

Major controversies and definition issues still exist about anastomosing rivers. It is still unclear why anastomosis forms and what the roles are of climate and base level (Makaske, 2001). Climate influences the water discharge, sediment load and the vegetation of the river. Certain controls of anastomosis (especially vegetation) differ with climate; however, modern anastomosing rivers have been reported from various climatic zones. Apart from climate, the influences of rapid base level rise and the effect of high floodplain sedimentation rates on anastomosis are still unclear. So, the exact origin of anastomosis is an unresolved matter. The aim of this research is therefore to explore what the origin of anastomosis is. In the present discussion about the origin of anastomosis, four hypotheses exist. The focus of this research is on the hypothesis proposed by Abbado et al. (2005) and Makaske et al. (2009). The other three hypotheses will be addressed in Chapter 2.

Hypothesis: Upstream control

Abbado et al. (2005) and Makaske et al. (2009) argued that the anastomosis of the upper Columbia River is caused by an upstream (excessive bed load supply) cause. They hypothesized that anastomosis of the upper Columbia River is generated from the inability of the river to transport its entire sediment load leading to in-channel aggradation and avulsions. So, excessive sediment supply is taken responsible for the origin of anastomosis. Furthermore, the upper Columbia River channels have no ability to migrate laterally, because of low stream power and erosion-resistant banks. This is caused by a low floodplain gradient and cohesive bank material. Because of the lateral channel stability, no lateral storage capacity for the surplus of sediment load is created. Therefore, much of the bed-material load is stored on the channel bed, leading to gradual decrease in flow capacity, increased overbank flooding and sedimentation, crevassing and cutting of new channels on the floodplain (Makaske et al., 2009).

To test the effect of the excessive bed load supply, the bed load input and output must be measured and the sedimentation rates over a longer period must be tested by collecting cores and radiocarbon dating from the floodplain sediment. This research will focus on the case of the upper Columbia River, whereby the hypothesis of upstream control will be tested by a fieldwork, by investigating the deposits and the long-term floodplain sedimentation rates of the upper Columbia River.

1.2 Research questions

Research questions associated with this study are:

- Is anastomosis a disequilibrium feature resulting from an overload of sediment on a low-energetic system?
- Is the network of multiple channels of the upper Columbia River stable and is it an equilibrium feature?

1.3 Research outline

The research questions are ideally explored through a process-based research as well as a geological reconstruction research. This was carried out during fieldwork in the upper Columbia River. The fieldwork took place for a period of 6.5 weeks, from August 18th till September 30th 2010. Tjalling de Haas and I collaborated in the collection of data in the field. Tjalling de Haas collected data for the process-based part of the project. He mapped the position of present multiple channels and measured widths, depths and bifurcation/confluence morphology in the field. He used the fieldwork results for a physics-based numerical model to investigate the evolution of the channel network under equal and aggrading conditions (De Haas, 2010). During my research, the long-term floodplain sedimentation rates are estimated, to assess whether the anastomosis of the upper Columbia River is caused by sediment overloading, or has another explanation.

The upper Columbia River consists of an upper reach where anastomosis is better developed than in the lower reach. My research aims to determine the relative importance of the external factor of the sediment dynamics in the Columbia Valley. To do this, the geological and lithological composition of the Columbia Valley is investigated, by making two floodplain-wide borehole cross-sections and by using AMS radiocarbon dating of macrofossils, wherefrom sediment budgets are derived. Two floodplain-wide borehole cross-sections were made, one in the upper highly anastomosing reach and one in the lower weakly anastomosing reach, to investigate if the long-term sedimentation rates in the upper reach are higher than in the lower reach. From this can be seen if indeed the differences in sedimentation rate are the driving force behind the differences in the rate of anastomosis. Those floodplain-wide cross-sections also make it possible to investigate if the network of multiple channels is stable over time, because former stages of the upper Columbia River become visible with cross-sections of the floodplain.

This thesis consists of a summarized overview of background information about anastomosing rivers and river sediment dynamics, a description of the fieldwork and a report of the gained results, with a discussion and conclusions.

2 General background

Prior to this MSc thesis, a literature review and a research proposal were written as an introduction to this research and to define the problem around the origin of anastomosis. That literature review consists of an extensive overview of existing literature about the classification of anastomosing rivers, the origin of anastomosing rivers and the upper Columbia River. In this chapter, a summary of the main points from this literature review is given. For more background information: see my literature review, or the cited references.

2.1 Site description

The upper Columbia River is located in south-east British Columbia, Canada within the Rocky Mountain Trench, an intermountain valley flanked by the Rocky Mountains on the north-east and the Purcell Mountains on the south-west (Figure 1). The source of the river is the Columbia Lake, from which the river flows in a north-western direction through the trench. Major tributaries to the upper Columbia River are the Bugaboo Creek and the Spillimacheen River, which drain the Purcell Mountains and supply sediment to the valley. The Purcell Mountains primarily consist of shales, sandstones, conglomerates and slates of Proterozoic age. The valley fill consists mostly of silts, sands and gravels, deposited during the Quaternary and are of glacial, glaciofluvial and glaciolacustine origin (Tabata and Hickin, 2003; Makaske et al., 2002).

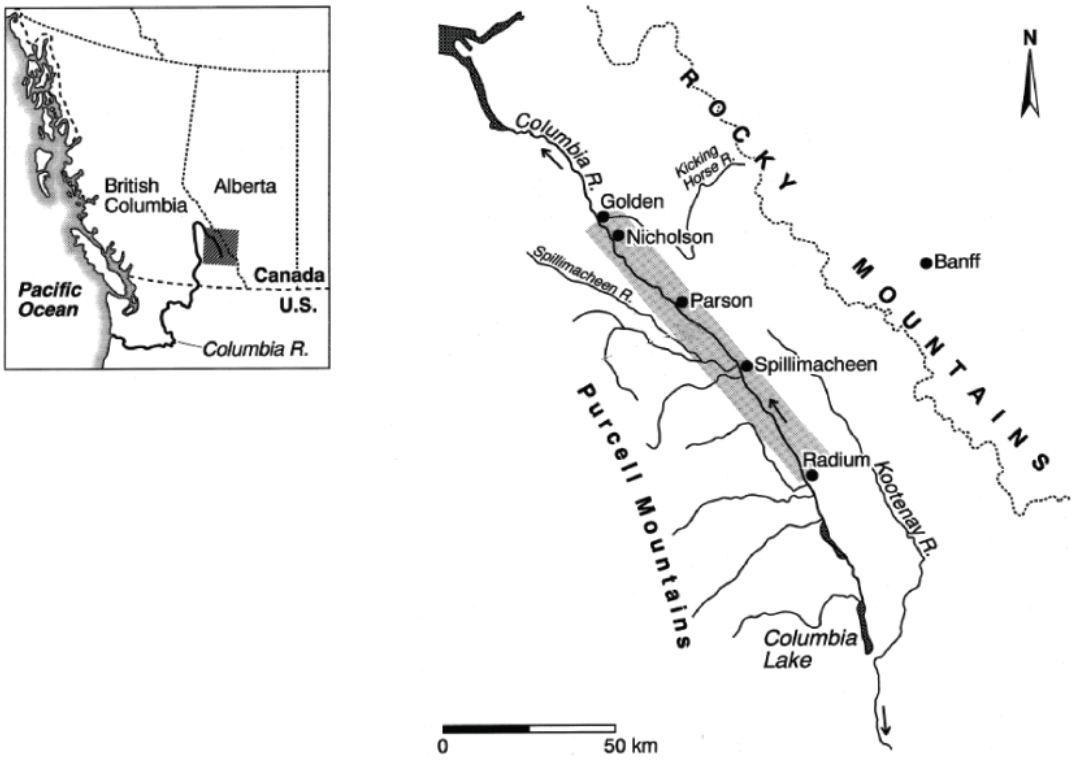

Figure 1. The location of the upper Columbia River in south-east British Columbia, Canada. The grey zone indicates the anastomosing reach of the upper Columbia River. During this research the area between Spillimacheen and Parson is studied (After: Makaske et al., 2002).

The anastomosing part of the upper Columbia River is located between Radium Hot Springs and Golden BC; this is a reach of about 120 km, with a mean floodplain width of 1.5 km (Figure 1). The upper Columbia River consists from Columbia Lake to Radium Hot Springs of a single channel. Downstream of Golden, the river consists of a braided channel with partly vegetated banks. The anastomosing morphology is best developed between Spillimacheen and Golden. At the confluence with the Spillimacheen River, near Spillimacheen, the upper Columbia River consists of a highly anastomosing reach of 15 km long, with three to five active channels. A 35-km-long weakly anastomosing lower reach with one to three channels is located between Castledale and Golden. The highly anastomosed upper reach is characterized by a relatively steep channel slope, a high number of crevasse splays, a high total crevasse splay-area/valley-area ratio and coarser bed material (Abbado et al., 2005).

The Columbia Valley has a humid continental climate with cold winters and warm summers. Water discharge in the upper Columbia River fluctuates seasonally in response to rainfall and snowmelt. Minimum discharge occurs during the winter, when there is an ice cover over the river. In the spring, snowmelt and rain cause a sharp rise in discharge with a peak in June and July. Bankfull conditions are reached almost yearly (Makaske et al., 2002). On average, overbank flooding occurs once a year for a period of 45 days (Locking, 1983). Mean annual water discharge is 108 m^3/s, bankfull discharge is 250 m^3/s and peak discharge is 300-350 m^3/s (Tabata and Hickin, 2003).

2.2 Definition and classification of anastomosing rivers

Anastomosing rivers are multiple channel systems on alluvial plains (Makaske, 2001, after Schumm, 1968). Anabranching rivers are also rivers with multiple channels, but have a wider range of river types. Anabranching is the division of a river by islands whose width is greater than three times water width at average discharge. A definition for anastomosing rivers is proposed by Makaske (2001): “An anastomosing river is composed of two or more interconnected channels that enclose flood basins”. At the scale of channel belts the terms ‘straight’, ‘meandering’ and ‘braided’ apply, whereas at a larger scale a river can be called anastomosing if it meets the definition given above. This means that straight, meandering and braided channels may all be part of an anastomosing river system. Nanson and Knighton (1996) classify river systems that consist of multiple channels separated by vegetated semi-permanent alluvial islands, formed by within-channel or deltaic accretion as anabranching rivers. They recognized six different types of anabranching rivers. The upper Columbia River as described by Makaske et al. (2002), Smith (1983), Tabata and Hickin (2003) and Abbado et al. (2005), is a type 1b anabranching river in the classification of Nanson and Knighton (1996). During this research, the upper Columbia River is referred to as “anastomosing”, as it exhibits resistant, well-vegetated banks that protect swampy, levee-banked islands, being the fundamental characteristics of type 1b anabranching mentioned by Nanson and Knighton (1996).

2.3 Hypotheses

The main hypothesis for the origin of anastomosis used in this research is proposed by Abbado et al. (2005) and Makaske et al. (2009), whereby an upstream control is taken as explanation for the anastomosis of the upper Columbia River. In the present discussion about anastomosis, three other hypotheses exist:

Hypothesis 1: Deltaic origin of anastomosis

A hypothesis about the origin of the anastomosing upper Columbia River is that the river is at a final stage, formed due to the deltaic infilling of lakes in the valley (Abbado et al., 2005, after Galay et al., 1984). Those lakes were formed due to ponding behind alluvial fans in the valley. The lakes were filled by river-dominated bird's foot deltas of which the anastomosing river system is a final stage. Lacustrine deltas can show the same characteristics of multiple channels as anastomosing rivers. Many deltas have a network of channels between bifurcations (channel splitting) and confluences (channel merging). Some of the distributaries of a delta have their origin in crevassing (Andrén, 1994), just like anastomosing rivers (Makaske, 2001). The formation of new channels can also be the result of channel splitting at channel mouth bars, whereby a bifurcation is formed during progradation of the delta (Smith et al., 1989). These mouth bars form at the mouth of distributaries, where diffusion and deceleration of the water flow takes place, which results in deposition of bed load and suspended load (Axelsson, 1967). Known examples of deltas with multiple channel systems comparable with the upper Columbia River are the Rhine-Meuse delta in the Netherlands and the Laitaure delta in Sweden (Axelsson, 1967; Andrén, 1994).

Hypothesis 2: Downstream control

The immediate cause of the frequent avulsions has been proposed to be a rise in base level (downstream control) (Smith, 1983). Large alluvial fans prograding into the valley have reduced the channel slope upstream in the upper Columbia River, whereby the capacity of the channel to transport the sediment is exceeded by the sediment supply. This causes an aggrading system which is supposed to be a necessary condition for anastomosis (Smith, 1983).

Hypothesis 3: Optimizing sediment transport

In another hypothesis anastomosing rivers are considered to be in equilibrium, where channels are adjusted in geometry and hydraulic friction to optimize transport of water and sediment discharges. In doing so, anastomosing rivers are able to concentrate stream power and shear stress in relatively narrow, deep, unobstructed channels. They maintain or increase sediment throughput, whereby a considerable advantage over a single-channel river is created (Huang and Nanson, 2000, 2007).

Hypothesis 1 proposed a deltaic origin of the anastomosis. To validate this hypothesis, deltaic morphologies must be found in the subsurface of an anastomosing river system. From geological

reconstructions, a prograding structure with mouth bars and lacustrine sediments must be found to prove this hypothesis.

To test the effect of the downstream control (hypothesis 2), the backwater adaptation length (λ_w) can be measured (which can be estimated as h/3S, whereby h is water depth and S is the slope of the channel). When the backwater adaptation length is large, this effect can not be neglected and it is possible that the anastomosis is the effect of a downstream control. In the case of the upper Columbia River λ_w= 11 km with $S = 9 * 10^{-5}$ and $h = 3$. This illustrates that a downstream control has an effect till 11 km upstream.

The origin of anastomosing rivers as proposed by Huang and Nanson (2000, 2007) is that channels are adjusted to optimize sediment transport (hypothesis 3). Tabata and Hickin (2003) tested the hydraulic efficiency of the upper Columbia River and found that channel splitting leads to hydraulic inefficiency. But there are not sufficient bed load transport measurements at bankfull flow available for the secondary channels of the upper Columbia River to specify the change in bed load transport capacity. Also, Tabata and Hickin (2003) used general friction relations, which make their results debatable. To test if optimizing sediment transport is the reason for a river to anastomose, more anastomosing rivers must be investigated including the upper Columbia River, to get better data of bed load transport capacity.

This research will test the hypothesis of upstream control of Abbado et al. (2005) and Makaske et al. (2009) by a fieldwork, by making a subsurface analysis. From this subsurface analysis, hypothesis 1 (deltaic origin) can also be tested.

2.4 Mechanisms leading to anastomosis

The mechanisms that actually produce anastomosing rivers appear to be a combination of two sets of different geomorphological processes (Makaske, 2001; Nanson and Knighton, 1996): (1) *Avulsion,* the process creating the pattern of multiple channel belts; and (2) *Processes determining channel morphology,* which ensure that the multiple channels can exist. The morphology of the individual channels is controlled by external factors as climate, bank material and geology.

Avulsion is the diversion of flow from an existing channel onto the floodplain, eventually resulting in a new channel belt (Makaske, 2001). Many avulsions are the result of the formation of a crevasse splay in a low-lying floodbasin. When a partial avulsion occurs, the new channel accommodates only a portion of the discharge of the older channel, whereby a system with multiple channels can be formed (Stouthamer, 2001).

Bridge and Leeder (1979, from Makaske, 2001) suggested that avulsion frequency increases with aggradation rate. The number of avulsions decreases when the rate of aggradation slows down (Makaske, 2001, after Törnqvist, 1994). The avulsion frequency is also controlled by the overall gradient of the floodplain. When the gradient is higher across the natural levee compared to the main channel,

favourable conditions for avulsion occur, because of gradient advantage. This gradient advantage is attained more easily on a low-gradient floodplain than on a high-gradient floodplain, because of the low channel gradients involved (Makaske, 2001).

If the floodplain is favourable for avulsion, a trigger is needed to start the avulsion. A large flood usually determines the timing of an avulsion (Makaske, 2001, after Brizga and Finlayson, 1990; Mack and Leeder, 1998). Other possible triggers are obstructions such as log jams, ice dams or beaver dams which block the discharge in the main channel, and forced the water to follow a new route, by starting a crevasse through the natural levee (Smith, 1983).

Anastomosing rivers maintain a multiple channel state by slow abandonment of old channels after the formation of bypasses by avulsions. Slow abandonment of old channels must occur at the same rate as the formation of new channels by avulsions to maintain a system with multiple channels. Slow abandonment of old channel segments is mainly determined by low stream power, caused by low-gradient floodplains. Strongly consolidated floodplain muds in combination with low stream power, allow only slow enlargement of channel-flow capacity of new secondary channel beds by bed scour and bank erosion. So when the secondary channels are not large enough to adjust to flood flows, the older channel has to carry a part of the peak discharge. This results in slow abandonment of older channels (Makaske, 2001). The lateral stability of individual channels in an anastomosing system is determined by cohesive, erosion-resistant banks and floodplains (consisting of clay and/or peat). For the formation of cohesive, erosion-resistant banks and floodplains, low stream power is needed to ensure the deposition of clay (Makaske, 2001). This low stream power is generally caused by a low floodplain gradient, which also prevents bank erosion.

In general, anastomosis is caused by a low floodplain gradient. A low gradient causes a low stream power. The specific stream power of the upper Columbia River is within the range for straight, laterally stable, channels (e.g. Van den Berg, 1995). In meandering rivers, bed load is stored in point bars, whereby the storage capacity is largely determined by the rate of lateral channel migration. Lateral accretion deposits (point bars) are lacking in straight rivers (Berendsen and Stouthamer, 2001). In a floodplain that is in equilibrium (neither increasing nor decreasing in volume), the loss of sediment by floodplain shaving by bank erosion and channel extension must be in balance with floodplain storage by overbank deposition and deposition in old channels and oxbow lakes (Lauer and Parker, 2008). In the upper Columbia River storage of bed load takes place on the channel bed. When the sediment supply is larger than the transport capacity, sedimentation will take place in vertical direction in the channel bed. When this aggradation rate is high, the avulsion frequency will increase (Jerolmack and Mohrig, 2007). Anastomosis appears to be the effect of disequilibrium between floodplain gradient and sediment supply. When the valley gradient would be in equilibrium with the sediment supply, the river would not be an aggrading

river, whereby the system is less favourable for avulsions, so a single channel system would probably occur.

The main channel is most liable to avulsion, because of a high in-channel aggradation rate (Makaske et al. 2009). The low specific stream power of the upper Columbia River indicates that little energy is available for lateral erosion of the cohesive loamy banks. The shallowing of the channels occurs if the bed aggradation exceeds the average natural levee growth rate. Secondary channels show negligible sediment transport rates, so in these channels bed aggradation does not exceed the natural levee growth. The secondary channels can exist for very long periods, because of slow channel infilling (Makaske et al., 2009).

Avulsions were common in the upper Columbia River, in the past 3000 years; nine new channels were formed by avulsion, while older channels were abandoned. The avulsion frequency of the upper Columbia River is therefore 3 avulsions/kyr (Makaske et al., 2002). This avulsion frequency is comparable to the avulsion frequency of the Rhine-Meuse delta (Makaske et al., 2002, after Törnqvist, 1994); showing that the upper Columbia River is not unique is its dynamics.

2.5 Sediment dynamics

To get better understanding of the sedimentation mechanisms of the Columbia River, the sediment load and dynamic sedimentation processes of the river must be studied. The classification of sediment load transported by rivers is based on the way the sediment is transported. This transport can take place in suspension (suspended load) or on the river bed (bed load). Sediment ending as bed-material load is transported partly in suspension and partly as bed load (Figure 2). Suspended load without interaction with the bed-material load is likely to be quickly 'washed' down the river, this is called wash load. So wash load is transported without being deposited on the river bed or contributing to morphological change. Bed-material load grains, on the other hand, continuously interact with the river bed and therefore can contribute to morphological change (Frings et al., 2008).

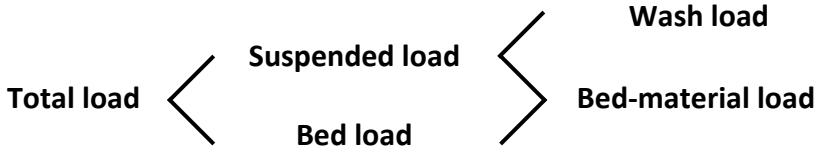

Figure 2. Classification of the sediment load transported by rivers (After: Frings et al., 2008).

2.5.1 Downstream fining in sand-bed rivers

A common phenomenon in sand-bed rivers is downstream fining of the bed sediments (Frings et al., 2008). Abbado et al. (2005) observed a statistically significant downstream fining in the reach between Spillimacheen and Golden. Four processes probably affect the downstream fining process in the upper Columbia River: 1) Overbank sedimentation can lead to a negative effect on the downstream fining

process, because the fine sediments become stored in the floodbasins. 2) Bifurcations can lead to a discontinuity in the grain-size distribution. 3) Sediment addition by tributary confluences can locally have a great effect on the grain-size distribution. 4) A high aggradation rate leads to a stronger downstream fining trend, because the coarse sediments become stored in the channel beds (Frings, 2007). It is hypothesized that the aggradation rate of the upper Columbia River is high and this will therefore cause a downstream fining trend. During this research, sediments in the upstream and downstream parts of the upper Columbia River are investigated with the subsurface analysis, wherefrom the grain-size distribution can be investigated.

2.5.2 Sediment budgets

From the sediment stored in a catchment, river responses to environmental changes (allogenic response) and autogenic controls (intrinsic response) can be derived. Two types of fluvial responses can be distinguished: 1) the geomorphic (-stratigraphic) response as reflected in the planform morphology and stratigraphic position; and 2) the sedimentary responses, which can be reconstructed from changes in the volumetric extent of the deposit. Erkens (2009) studied the fluvial response of the Rhine-Meuse delta. He qualitatively determined the geomorphic response by analyzing palaeogeographic maps and cross-sections, whereas the sedimentary response was quantitatively investigated within a sediment budget framework.

This research yielded comparable data as the study of Erkens (2009), which makes it possible to study the fluvial response of the upper Columbia River in a comparable way. This study considers the upper Columbia River as a sediment trap, just as Erkens (2009) did for the Rhine-Meuse delta. The stored volume of sediment is the difference between input (sediment delivery) and output (dependent on the trapping efficiency). Input, output and change in sediment storage (sedimentation, erosion) for a certain catchment can be solved over a unit of time. Sediment storage depends on the sediment input and the trapping efficiency. The sediment storage will be large with a relatively large sediment input and with a large trapping efficiency. Sediment stores are classified in three different stores: 1) in-channel: channel lags and channel fill; 2) overbank: levee and floodplain; and 3) abandoned channel fill deposits. Erkens (2009) analyzed trends in sediment deposition in suspended load and bed load. This would be called wash load and bed-material load in the process-based classical division as presented by Frings et al. (2008). During this research, this classical division will be used, whereby in-channel and abandoned channel fill deposits are assumed to consist of bed-material load and overbank deposits of wash load. By analyzing the cross-sections of a sediment trap, trends in deposition in wash load and bed-material load are gained. When age information is available in the cross-section, the sediment storage can be resolved over time. This gives the opportunity to compare sediment budgets at different locations in the valley. These sediment budgets are representative for a time scale of thousands of years. To compare these results with modern sediment measurements, one must known if the sedimentation rates in the past are

comparable with these from the present. Ten Brinke et al. (2000) published recent sediment budgets measurements for the river Rhine. Compared to the long-term sediment budget estimates of Erkens (2009), they turn out to be of the same magnitude. Here it is therefore assumed that the long-term and recent results of sedimentation rates of the upper Columbia River are also comparable.

2.5.3 Sedimentation rates

Makaske et al. (2009) estimated the sediment budgets of bed load deposition for the upper (highly) and the lower (weakly) anastomosing reaches of the upper Columbia River. Based on the hydraulic and sediment transport data from Locking (1983), bed load input into the upper anastomosing reach during bankfull discharge is estimated at 7.1 kg/s (1.27 * 10^5 m^3/yr, assuming a dry bulk sediment density of 1770 kg/m^3). Makaske et al. (2009) estimated the bed load transport in his studied floodplain-wide cross-section near Castledale (Figure 3 and Figure 4) by using the sediment transport predictor of Van Rijn (1984). He found bed load transport rates during bankfull discharge in the range of 1.2-3.3 kg/s (2.14-5.88 * 10^4 m^3/yr). Near Nicholson, bed load output from the lower anastomosing reach at bankfull discharge is estimated at 0.6 kg/s (1.07 * 10^4 m^3/yr) (Figure 3). According to these numbers 58-91% of the bed load is stored in the reach between Spillimacheen and Castledale and 9-42% is trapped in the lower anastomosing reach (Figure 3) (Makaske et al., 2009). For the upper anastomosing reach, the bed aggradation rates in the main channel (15 km long, 100 m wide) are 13.3-20.9 mm/yr (2.00-3.14 * 10^4 m^3/yr), based on the deposition rates of Figure 3. For the lower anastomosing reach, main channel bed (35 km long, 100 m wide) aggradation rates between 0.9-4.1 mm/yr (3.11-14.5 * 10^3 m^3/yr) were

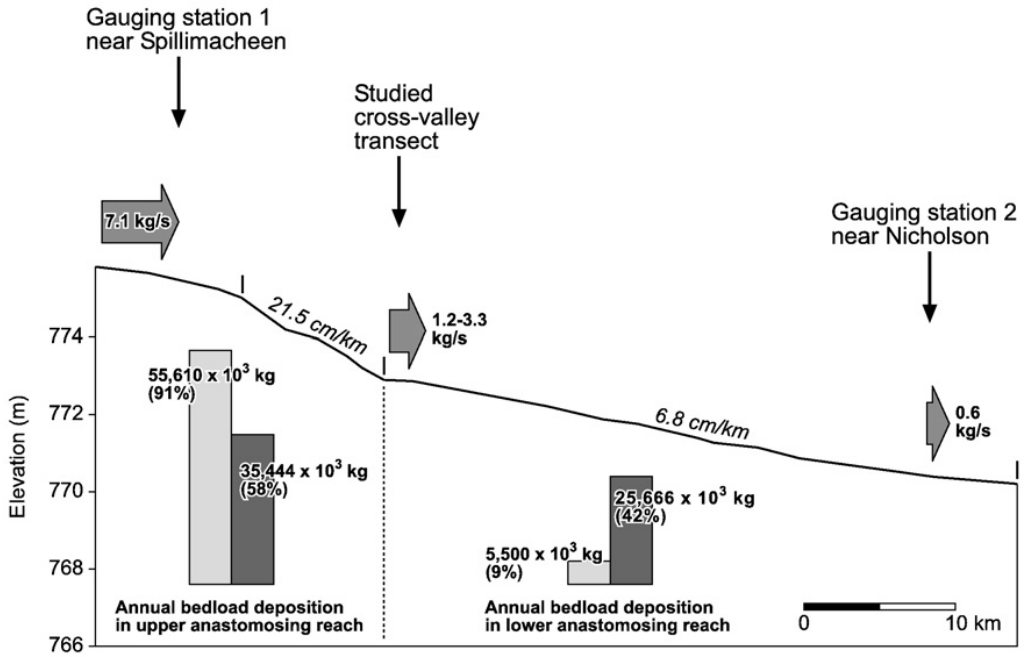

Figure 3. Longitudinal profile of the upper Columbia River main channel, showing in downstream direction (left to right) a gentle upstream reach, a steep reach and a gentle lower reach. Light grey bars represent scenario with maximum difference between sediment storage in upper and lower anastomosing reach, dark grey bars represent scenario with minimum difference between sediment storage in upper and lower anastomosing reach. The location of the studied floodplain-wide cross-section is displayed in Figure 4 by the transect of Castledale (From: Makaske et al., 2009).

calculated by Makaske et al. (2009). Channel shallowing is still likely to occur in this reach, but at an absolute slower rate than in the upper anastomosing reach, because the bed load input in this reach is much lower than in the upper reach (Makaske et al., 2009).

The long-term average floodplain sedimentation rate of the upper Columbia River at the location of the floodplain-wide cross-section near Castledale is 1.75 mm/yr. Radiocarbon ages were used to calculate long-term sedimentation rates (Makaske et al., 2002). The upper Columbia River is not unique in this; the Rhine-Meuse delta for example has an average floodplain sedimentation rate of 1.5 mm/yr (Makaske et al., 2002, after Van Dijk et al., 1991) and the Saskatchewan River has an average floodplain sedimentation rate of 1.3 mm/yr (Makaske et al., 2002, after Morozova and Smith, 1999). Those rates are based on groundwater gradient lines (Rhine-Meuse delta) and on an average peat and organic-rich sediment growth rate (Saskatchewan River). The latter might underestimate average floodplain sedimentation rate, therefore Smith (1983) suggested an average of 1.5 mm/yr for the Saskatchewan River. Those are all relatively rapidly aggrading fluvial systems with multiple co-existing channel belts. The long-term average floodplain sedimentation rates in the upper and the lower anastomosing reach are not investigated. Therefore, they will be investigated during this research, to test the hypotheses that the long-term average floodplain and in-channel sedimentation rates in the upper anastomosing reach are higher than in the lower anastomosing reach.

3 Methods

The floodplain of the Columbia Valley is formed under influence of large amounts of sediment input, a yearly varying difference in water discharge and tributary alluvial fans, influencing the gradient and width of the floodplain. This chapter will present the methods used to get a better understanding of the sediment dynamics in the Columbia Valley. The geological and lithological composition of the Columbia Valley was therefore investigated. In this study the results of Makaske et al. (2002) and Makaske et al. (2009) are used in the interpretation of the new field data.

3.1 Fieldwork

The fieldwork in the Columbia Valley was carried out in a period of 6.5 weeks. About 4 weeks were available for this part of the project and about 2 weeks for the project of Tjalling de Haas. The first week Dr. A. Makaske accompanied us in the field, and the first day Prof. D.G. Smith helped us start up in the field. Two floodplain-wide transects were investigated as addition to the investigated transect near Castledale of Makaske et al. (2002). The location of the transects was chosen in order to 1) obtain evenly-spaced cross-sections oriented perpendicular to the general flow direction; and 2) cross both the highly (lower) and weakly (upper) anastomosing reach of the Columbia Valley. The transect investigated by Makaske et al. (2002) near Castledale is located in between the two investigated transects of this study. The spacing between the transects is about 17 km. The locations of the two new transects are near Harrogate and Parson (Figure 4). The exact locations of the transects were determined in the field based on the accessibility. The location of the transect near Harrogate is in the upper anastomosing reach of the river. At this point of the river floodplain, five channels are active during high water and two residual channels are located on the floodplain. This transect could be reached by boat. The second transect is located along an elevated road at Parson and is located in the lower anastomosing reach of the river. The elevated road crosses the floodplain and has five bridges in the dam. The Parson transect crosses two active channels and two residual channels. During the period of the research on this second transect, the water depth in the upper Columbia River was too low to use the boat, therefore a location was chosen whereby the transect could be reached easily from the road without a boat.

In the transects, floodplain-wide borehole cross-sections were made. The borings were carried out using an Edelman auger for sediments above the groundwater level and a gouge for the sediments below the groundwater level (Figure 5A) (Makaske et al., 2002, after Oele et al., 1983). As a gouge performs poorly in water-saturated sandy sediments, two cores were collected with a vibracore. Those vibracores were performed in the sandy channel-filling in the Harrogate transect, using the equipment described by Smith (1984, from Makaske et al., 2002) (Figure 5B). On every drilling site, the boreholes were made as deep as possible, which was usually between 5 to 8 m. The locations of the boreholes were determined by morphological variations in the field. The borings were placed in floodbasins, on natural levees and in residual channels (Appendix 2, Appendix 3). The exact location of the boreholes was measured with a

Figure 4. Locations of the transects in the Columbia Valley. Transect Harrogate and transect Parson are investigated during this research, transect Castledale during the research of Makaske et al. (2002). In yellow Road 95 is displayed and the arrow near Harrogate indicates the flow direction of the upper Columbia River. The Spillimacheen River enters the Columbia Valley in the lower left corner of the picture (Image from: Google Earth).

Global Positioning System. The sediments from the cores were logged in the field at 10 cm intervals (Appendix 1). This involved a description of texture, organic matter content, gravel content, median grain-size, color, oxidized iron content, occurrence of groundwater and other characteristics, such as the occurrence of shells and plant remains (cf. Berendsen and Stouthamer, 2001). The elevation of the boring locations was determined by leveling the floodplain over the whole transect. The elevation was leveled relative to an arbitrary datum with a leveler on a tripod and a leveling rod. The depth of the channels

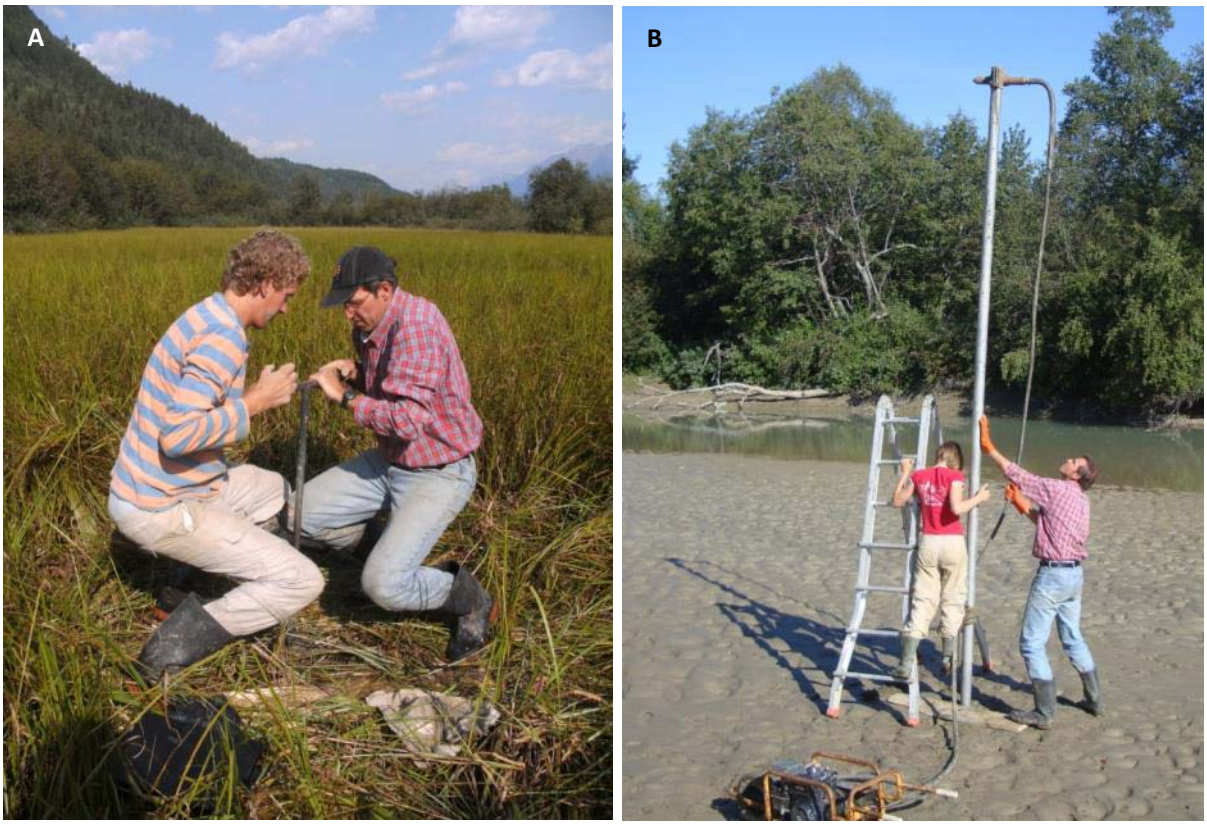

Figure 5. A: Boring in a floodbasin, using a gouge. B: Boring in a residual channel, using a vibracore.

in the transect of Harrogate was measured with an echo sounder, mounted on an inflatable boat with outboard motor. This was not possible in the transect of Parson, because the water stage was too low to use the boat. Therefore the depth of the main channel in the transect of Parson was estimated by using the interchannel hydraulic geometry relationships as derived by Tabata and Hicking (2003):

$$W = 3.24\ Q_{bf}^{0.64} \quad (1)$$

$$h = 1.04 Q_{bf}^{0.19} \quad (2)$$

wherein *W* is the width of the channel, measured in the field. From that the bankfull discharge Q_{bf} can be derived whereafter width-averaged water depth *h* can be calculated. This gives a water depth similar to the hydraulic geometry relationships of De Haas (2010), within a range of a factor 2. The depth of the other channels in the transect of Parson was measured with a core extension rod.

3.2 Lithological borehole cross-sections

The borehole descriptions were used to make two floodplain-wide cross-sections of the upper Columbia River floodplain. The borehole descriptions were entered in the computer programme LLG 2008, which is a borehole data programme. This programme is able to plot the borings on a depth/distance plot. The borings were numbered with the group name 400991 preceding the borehole number. The borings were not all in a perfectly straight line perpendicular to the general flow direction (Appendix 2, Appendix 3). This could result in an overestimation of the width of the morphological elements in the cross-sections. Therefore, the line connecting the boring locations was on some locations adjusted to a line perpendicular

to the general flow direction. This was carried out for boring 010, 011 and 058. By making the cross-sections, the principles described by e.g. Berendsen and Stouthamer (2001) were used to determine lithogenetic units from the obtained lithological information. By these principles, a channel belt in the floodplain has adjacent natural levee deposits and floodbasin deposits that correlate to the channel belt.

3.3 Genetic interpretation of the borehole cross-sections

The lithological borehole cross-sections were used to make a genetic interpretation of the sediments in the cross-sections. Four different genetic groups were used to classify the fluvial sediments. Those are: floodbasin deposits and peat, levee deposits, channel deposits and crevasse splay deposits. The non-fluvial and alluvial fan deposits were indicated together in a separate group. Lithological and morphological characteristics of the sediment bodies are used for the genetic classification. Sand bodies which are relatively deep and narrow were classified as channel deposits. Sand bodies which are less deep than channel sand bodies more outspread and with no direct link to a channel were classified as crevasse splay deposits. Natural levee deposits are wedges of loamy deposits attached to the upper part of channel sand bodies. Levees are formed by overbank deposition. Floodbasin deposits consist of clay, silty clay and peat and are located in between channel sand bodies. Floodbasin deposits are deposited during floods. The non-fluvial deposits consist of colluvium from the bedrock and regolith and the alluvial fans are lateral fan input in the valley.

By making the genetic interpretation of the lithological cross-sections, it became clear that more interpretations were possible about the genesis of the sediment in the cross-section. Makaske et al. (2002) made a detailed genetic interpretation of the cross-section near Castledale. Small units with a different lithological composition than the surrounding material were marked as a separate unit. But it is also possible to interpret the lithological profiles in a more general way. Therefore, it was chosen to make two versions of the genetic interpretation of the three borehole cross-sections. This was done to show the different ways in interpretation and to test if there are significant differences in the total proportions of the different genetic classes by both methods. Version 1 includes the interpretation of the Castledale cross-section of Makaske et al. (2002) and an interpretation of the Harrogate and Parson cross-sections on a comparable detailed way. Version 2 includes the more general interpretation of the profiles; this version also contains a reinterpretation of the Castledale cross-section.

3.4 Aerial photographs used to obtain trends in sediment deposits

Aerial photographs of Google Earth were used to obtain a trend in the different kinds of geomorphological units along the river. The visible geomorphological characteristics of the floodplain are classified in the same four classes as the sediments in the cross-sections: floodbasin, levee, channel and crevasse splay. This was done by printing the images on a large scale; whereafter this print was used to measure every 3 km perpendicular to the flow direction the width of the geomorphological elements in

the floodplain with a ruler. In this way, 20 transects were measured, from the Spillimacheen River to 10 km downstream of Parson. Based on these measurements, the proportions of floodbasin, levee, channel and crevasse splay morphologies were derived.

3.5 Channel chronology

Makaske et al. (2002) used ^{14}C dates to make an estimate of time periods of activity of active channels and paleochannels in their studied transect near Castledale. This is not possible for this research, because of a lack of dateable organics at suitable stratigraphic position. Therefore the cross-sections were used to make a graph of the distribution of channels in depth in the cross-sections, to analyze if there are trends in periods with more and less channel activity. To do this, the depth of the channel sand bodies and the depth of the bases of levees are measured. The depths of the channel sand bodies give the distribution of the channels in depth and an estimate of the end phase of channel activity. The depths of the levee bases give the beginning of sedimentation and so the beginning of channel activity. By plotting all tops of channel sand bodies and levee bases of one transect in a graph, it becomes visible if the distribution of channels is equally over depth or shows clusters. This distribution can thereby tell something about the channel activity over time. These graphs of depths of tops of channel sand bodies and levees bases were made for the three transects to analyze the trend of channel chronology in downstream direction.

3.6 AMS radiocarbon dating of macrofossils preparation

Precise time control is essential to determine the sedimentation rates in the upper and lower anastomosing reach. During this research ^{14}C dating of macrofossils by using accelerator mass spectrometry (AMS) was applied. These macrofossils were extracted from cores from boreholes. Macrofossils are most useful, since they are relatively unlikely to record disturbances in age as contamination by roots, hard water effect or reworked organic material (Törnqvist et al., 1992). The samples were taken from floodbasin peat and humic clay at great depth (6-7 m) to enable calculation of long-term sedimentation rates. The sediments in the Columbia Valley floodplain are not rich in organics: only four borings, two in each cross-section, were useful. These borings were re-bored with a thicker gouge (6 cm Ø instead of 3 cm Ø) (Figure 6). From those cores, 14 samples were taken from carefully

Figure 6. Gouge used for taking samples for dating of macrofossils. Exact depth measured using a measuring tape.

measured depth. After the field description, the samples were removed from the gouge with a knife and put into a sealing bag and stored in a refrigerator. Five samples were selected for AMS radiocarbon dating. These samples were chosen because of their high organic matter content and great sampling depth. One of the five samples was taken at a shallower position to investigate potential long-term variability in sedimentation rate. Floodplain stratigraphy did not allow taking more shallow samples. The sample locations are indicated in Appendix 4 (boreholes 003, 029, 051 and 055). Below, the description of the preparation of the macrofossil samples for AMS radiocarbon dating is given:

- The samples were cleaned of all potentially allogenic material with a knife and cut into slices of 2 cm.
- To disaggregate the sediment, the slices of the samples were transferred into a beaker to which a 5% KOH solution was added.
- To stimulate the disaggregation of the sediment, the beakers were covered with a watch glass and placed on a hotplate of 90°C for one hour.
- To collect the organics, the samples were sieved over a 150 µm mesh sieve, after almost all sediment was disaggregated.
- To avoid rotting of the organics, the sediment stored in the sieve was cleaned with distilled water and put into a plastic sealed bag with a drop of a 5% HCL solution.
- To search for dateable macroscopic residues in the organics, the solution with the organics was placed under a microscope in a petri dish. All dateable residues were picked out with a tweezer.
- After that, the dateable residues were described and collected in a tube with distilled water and a drop of a 5 % HCL solution.
- In order to clean the terrestrial macrofossils, the carbonates on the terrestrial macrofossils must be dissolved. Therefore, the water in the tubes was drained with a pipette and replaced by a 5% HCL solution. After this, the tubes were placed in a stew for one hour on 70°C to stimulate the reaction.
- To remove the 5% HCL solution, the tubes were drained with a pipette and refilled with distilled water; this process was repeated three times.
- To check the terrestrial macrofossils, the tubes were emptied in a petri dish and placed under the microscope. If necessary, the terrestrial macrofossils were cleaned by using a tweezer. After that the terrestrial macrofossils were collected in a cleaned tube.
- To dry the terrestrial macrofossils, the tubes were placed in a stew for one night at 70°C.
- After this, the dried residues were labeled (Table 1) and ready to send in for dating. The samples were named after the location, sample number and depth below surface. Sample 2.2A for example was sent in under the name Harrogate 2.2A 421-423.

Table 1. Selected macrofossils, send in for dating. Sample numbers correspond with the sample numbers in Appendix 4 except of the addition of "2.", added to make difference with the numbering of Makaske et al. (2002). The letter indicates which part of the core sample is selected for dating.

Location	Sample	Depth below surface (cm)	Borehole number	Material
Harrogate	2.2A	421-423	003	4 *Carex rostrata* type, 12 *Carex aquatilis*
Harrogate	2.7C	644-646	003	23 *Betula*, 2 *Myrica*
Harrogate	2.8B	670.5-673	029	1 *Viola* sp., 1 *Schoenoplectus lacustris*
Harrogate	2.8A	668.5-670.5	029	2 *Coniferae,* 3 *Carex rostrata type,* 1 *Carex* sp., 2 *Schoenoplectus lacustris*, 2 *Betula*
Parson	2.12E	554-556	055	1 *Carex paniculata* group, 2 *Carex rostrata* type, 3 *Carex* sp., 1 *Rosaceae*, 2 *Galium* sp.
Parson	2.12D	552-554	055	4 *Salix,* 2 *Carex rostrata* type, 5 *Carex* sp.
Parson	2.14D	522-524	051	25 *Schoenoplectus lacustris*, 2 *Carex rostrata* type, 3 *Carex paniculata* group, 9 *Carex* sp., 3 *Carex*

3.7 Sediment dynamics

To test the idea that excessive sediment supply causes a higher aggradation rate in the upper anastomosing reach than in the lower anastomosing reach, three methods were used to get insight into the sediment dynamics:

1) Measured sediment transport values of Locking (1983) and sediment transport predictions of Makaske et al. (2009) were used to calculate the sedimentation rate.
2) Sediment transport predictors were used to calculate the sedimentation rate.
3) The genetic interpretation of the borehole cross-sections were used to make an estimate of the sedimentation rate, whereby AMS radiocarbon dates will be used later.

The deposition area was split up into two regions: an upper, highly anastomosing reach from Spillimacheen to Castledale and a lower, weakly anastomosing reach from Castledale to Nicholson. The upper reach is 15 km long, with a floodplain surface of 19.59 km^2. The lower reach is 35 km long and has a floodplain surface of 45.71 km^2.

3.7.1 Sediment transport measurements and predictors used to obtain sedimentation rates

Locking (1983) measured the suspended and bed load transport rates upstream of the highly anastomosing reach and downstream of the weakly anastomosing reach. From the measurements of Locking (1983) the sediment deposition in the total area could be calculated by taking the difference between sediment input and output. The data of Locking (1983) is published in tonnes/yr; this is converted to m^3/1000yr. A ton is taken as 1000 kg, as given in Locking (1983). The conversion from kg to m^3 was made with a dry bulk density of 1770 kg/m^3 for bed load and 1300 kg/m^3 for suspended load. The

published data is given in years; this is converted to 1000 yr, by making the assumption that the data of Locking (1983) is representative for a longer period. The sediment deposition in m^3/1000yr was used to calculate the accumulation rate in mm/yr, by dividing total sediment deposition with the total floodplain deposition surface. It is not possible to calculate the sediment deposition in the separate areas of the upper and lower anastomosing reach from these data. So, only the sedimentation rates for the total area are given. The sediment transport measurements of Locking (1983) are considered by her as suspended load and bed load measurements. During this research, that suspended load is taken as wash load, because Locking (1983) investigated that her suspended load concentration almost totally consist of wash load. This is confirmed by Whetten et al. (1969), who measured sediment grain size in the Grand Coulee Reservoir, which traps sediment from the upper Columbia River, the Kootenay River and the Clark Fork River. That reservoir is filled with very fine sediments, transported as wash load. This is caused by the sediment sources that produce generally fine-grained sediments, such as the clays and silts from the glaciolacustrine sediments and loess deposits (Whetten et al., 1969; De Haas, 2010).

Makaske et al. (2009) used the sediment transport measurements of Locking (1983) in combination with sediment transport predictions to calculate the sediment deposition in the separate areas of the upper and lower anastomosing reach from this date. They used sediment transport predictors to calculate the amount of bed load transport near Castledale. These results combined with the results of Locking (1983) give an estimate of the total amount of bed load deposited in the two sub-reaches of the floodplain. During that calculation, the Van Rijn (1984) bed load predictor was used, with a period of bed load transport of 108 days per year, as observed by Locking (1983).

3.7.2 Sediment transport predictors used to obtain sedimentation rates

From all data collected by Locking (1983), Makaske et al. (2002), Tabata and Hickin (2003) and Abbado et al. (2005) and the aerial photographs of Google Earth it was possible to calculate the sediment transport rate at different locations in the river system. The Van Rijn predictor for bed and suspended sediment transport rate is used by De Haas (2010) to compare the amounts of bed and suspended sediment transport, which indicated that the upper Columbia River is a bed load dominated river. This implicates that the sediment transport rate in the upper Columbia River can be modelled by using a bed load transport predictor only. Bed load transport (Q_b in m^3/s) was predicted with the Van Rijn (1984) predictor and with a bed load predictor which is fitted by De Haas (2010) on the sediment transport rates measured by Locking (1983). Bed load transport was predicted at Spillimacheen, Castledale and Nicholson to compare with the results of Makaske et al. (2009). Bed load transport was also predicted for three representative locations at the different anastomosing reaches: 1) for the middle of the reach between Spillimacheen and the steep reach (upstream gentle reach); 2) for the middle of the highly anastomosing steep reach and 3) in the weakly anastomosing gentle reach near Parson. It is chosen to make a prediction

at the upstream gentle reach because this determines the inflow of sediment in the steep reach. For the location of the reaches with different gradients see Figure 3.

Fixed parameters

Based on hydraulic data measured by Locking (1983), the value of the Chézy parameter can be calculated for both Spillimacheen and Nicholson. The Chézy parameters for Spillimacheen and Nicholson are respectively approximately 54 and 28 $m^{0.5}/s$ for bankfull discharge, corresponding to a roughness length k_s of 0.03 m and 1.2 m. For the calculations of the bed load transport a k_s of 0.15 m was used as an approach for all locations (De Haas, 2010).

The D_{50} and D_{90} measured at Spillimacheen are respectively 7.1 * 10^{-4} m and 1.8 * 10^{-3} m, and at Nicholson respectively 4.7 * 10^{-4} m and 8.7 * 10^{-4} m. As an estimate, the values at Spillimacheen were used. The slope at a certain point was taken as an average for the reach the point is located on. This was calculated with the elevation measurements of Abbado et al. (2005) (De Haas, 2010).

Data

Locking (1983) measured width and depth of the channels at various stages, while it is not clear which values indicate bankfull discharge. If possible, bankfull depth and width measured by Makaske et al. (2002), Abbado et al. (2005) or Tabata and Hickin (2003) were used. At Nicholson and Parson the bankfull channel width W_{bf} was measured by using the aerial photographs of Google Earth, and its corresponding bankfull water depth h_{bf} was calculated from hydraulic geometry

$$W_{bf} = 4.25\, Q_{bf}^{0.56} \quad (3)$$

$$h_{bf} = 0.99 Q_{bf}^{0.23} \quad (4)$$

wherein Q_{bf} is bankfull discharge. This hydraulic geometry relationship is different from the one of Tabata and Hicking (2003) which is used during this research to determine the depth of the channels in the transect of Parson (equation 1 and 2). The cross-sections were already drawn with channel depths related from the equations of Tabata and Hicking (2003), before De Haas (2010) developed the new hydraulic geometry given above and therefore, both relationships are used during this research. The slope at each transect was calculated by using elevation data of Abbado et al. (2005). They measured the slope only in the main channel, so for the secondary channels the same slope was assumed. During the calculations, the mean slope of each reach was taken.

Procedure

Hydraulic radius *R* is given as

$$R = \frac{Wh}{W+2h} \quad (5)$$

where *W* = channel width and *h* = water depth. The Chézy coefficient *C* is

$$C = 18\, log \frac{12R}{k_s} \quad (6)$$

where k_s is 0.15 m. From this velocity u can be calculated.

$$u = C\sqrt{RS} \tag{7}$$

where *S* is the slope. For bed load transport predictors the grain-related shield stress θ' is needed:

$$\theta' = \frac{u^2}{C^2(s-1)D_{50}} \tag{8}$$

wherein

$$s - 1 = \frac{\rho_s - \rho}{\rho} \tag{9}$$

with ρ is the density of water (1000 kg/m^3) and ρ_s is the facies mass density (2650 kg/m^3). Then the nondimensional sediment transport rate was calculated by a bed load transport predictor, fitted by De Haas (2010) to the sediment transport data of Locking (1983):

$$\emptyset_b = 5.62(\theta')^{1.66} \tag{10}$$

And also with the Van Rijn (1984) bed load predictor:

$$\emptyset_b = 0.1\left(\frac{\theta' - \theta_{cr}}{\theta_{cr}}\right)^{2.1} D^{*-0.3} \tag{11}$$

where θ_{cr} is the critical shield stress (here: 0.03) and where

$$D^* = D_{50}\sqrt[3]{\frac{(S-1)g}{\upsilon^2}} \tag{12}$$

where g = acceleration due to gravity (9.81 m/s^2) and υ = kinematic viscosity of water. Here υ = 1.0 * 10^{-6} was used. Unit bed load sediment transport rate was then calculated with the nondimensional sediment transport rate

$$\emptyset_b = \frac{q_b}{\sqrt{(S-1)g}D_{50}^{3/2}} \tag{13}$$

wherein q_b = unit bed load sediment transport rate (m^2/s). Finally total bed load transport rate was calculated as

$$Q_b = q_b * W \tag{14}$$

The total bed load transport rate was used to observe differences in transport between the different parts of the anastomosing reach. It is also used to calculate the sedimentation in the reaches. This is possible, because the differences between input and output give the storage or erosion in the area. This sedimentation rate in m^3/s can be converted to m^3/1000yr and therefore can be compared with the data of Locking (1983) and Makaske et al. (2009). During the calculations, the bankfull discharge was used. However, the upper Columbia River discharge is characterized by a highly seasonal discharge. To overcome the large discharge variability, channel forming discharge must be used. The channel forming discharge is calculated by De Haas (2010) by using discharge data from the Nicholson gauging station and the flow and sediment transport data of Locking (1983), wherefrom a discharge-unit sediment transport rate relation is derived. The calculated channel forming discharge is 187 m^3/s.The amount of bed load transport for bank full conditions is three times higher than for the channel forming discharge. Therefore, the total amount of bed load transport was divided by three, to obtain the yearly transport.

3.7.3 Genetic profiles and AMS radiocarbon dates used to obtain sedimentation rates

To investigate the differences between the genetic profiles, the total area of the different genetic classes (floodbasin, channel, levee and crevasse splay) was determined. This was done by plotting a grid with uniform boxes over the profiles. After that, it became possible to count all boxes and to quantify the total surface of the classes for both versions of interpretation of the genetic profiles. These surfaces were used as an estimate for the long-term sedimentation rate. These rates were calculated for wash load and for bed-material load. Levee deposits and floodbasin deposits were taken together as wash load and crevasse splay deposits and channel deposits were taken together as bed-material load. The volumes of organic deposits were neglected and added to the floodbasin deposits (wash load), because of the small amount of those deposits. The total area of the profiles was taken as an estimate for 3000 years of deposition. This is based on the AMS radiocarbon dates of the sediment in the transect of Harrogate, Castledale and Parson. In those cross-sections an age of 3000 years can be taken as a rough estimate for the total deposition of the cross-sections. The surface areas of profile of Harrogate was taken as a representative estimate of the sedimentation rate for the highly anastomosing reach and the profile of Parson was taken as a representative estimate for the lower anastomosing reach. The total area of the surface of both reaches was used to calculate the sedimentation of wash load and bed-material load per m^3/1000yr. From this, the sedimentation rate was calculated in mm/yr. On places where a morphological element did not have a realistic area size, a correction is applied. This is needed because when the transect line is not perpendicular to a morphological element, the measured surface of the element is not the real surface. This can lead to a wrong proportion of the measured surfaces of the different genetic classes. This correction is applied in the profile of Parson, because there was an unrealistic large sand body.

However, by assuming a deposition period of 3000 years for both Harrogate and Parson, less variation in sedimentation rate is assumed. It is possible to improve this by using the AMS radiocarbon dates. Unfortunately, not enough time was available to perform those calculations to the sediment budgets of the genetic profiles. Therefore the AMS radiocarbon dates are only used to calculate the total volume of sedimentation in m^3/1000 yr after calculating the average sedimentation rate. Those results are thereafter compared this with the results of the budgets estimated from the genetic profiles. So, sedimentation rates from the budget calculations from the profiles and from the AMS radiocarbon dates are used as two independent methods for analysing a downstream trend in sedimentation rates. Additional research is possible to integrate those two.

4 Results

4.1 Sedimentary environments and morphogenesis of the anastomosing river system

Six sedimentary environments of the upper Columbia River and associated lithofacies were identified by Smith (1983); channels, natural levees, crevasse splays, marshes, lakes and mires. In this section these sedimentary environments will be illustrated by pictures from the field, with the marshes, lakes and mires taken together as floodbasin deposits.

Figure 7 gives a view on a representative part of the upper anastomosing reach of the upper Columbia River. In the upper right corner of the photograph, an alluvial fan enters the valley (A). The floodplain is bounded by a road in the upper part of the picture (east) (B), the west part of the floodplain is fenced off by the mountain range, from where the picture is taken (C). In the middle of the picture, a sandy, non vegetated crevasse splay is visible (D). This is a young splay, formed by a levee break of the main channel. The crevasse cuts through a residual channel (E). This residual channel is recognizable by the line of trees on the levees of the channel. The floodbasins are partly filled with water on the moment of taking of the picture (end of August). Below the crevasse splay, an outflow channel is formed to transport the water from the floodbasins to the channels (F).

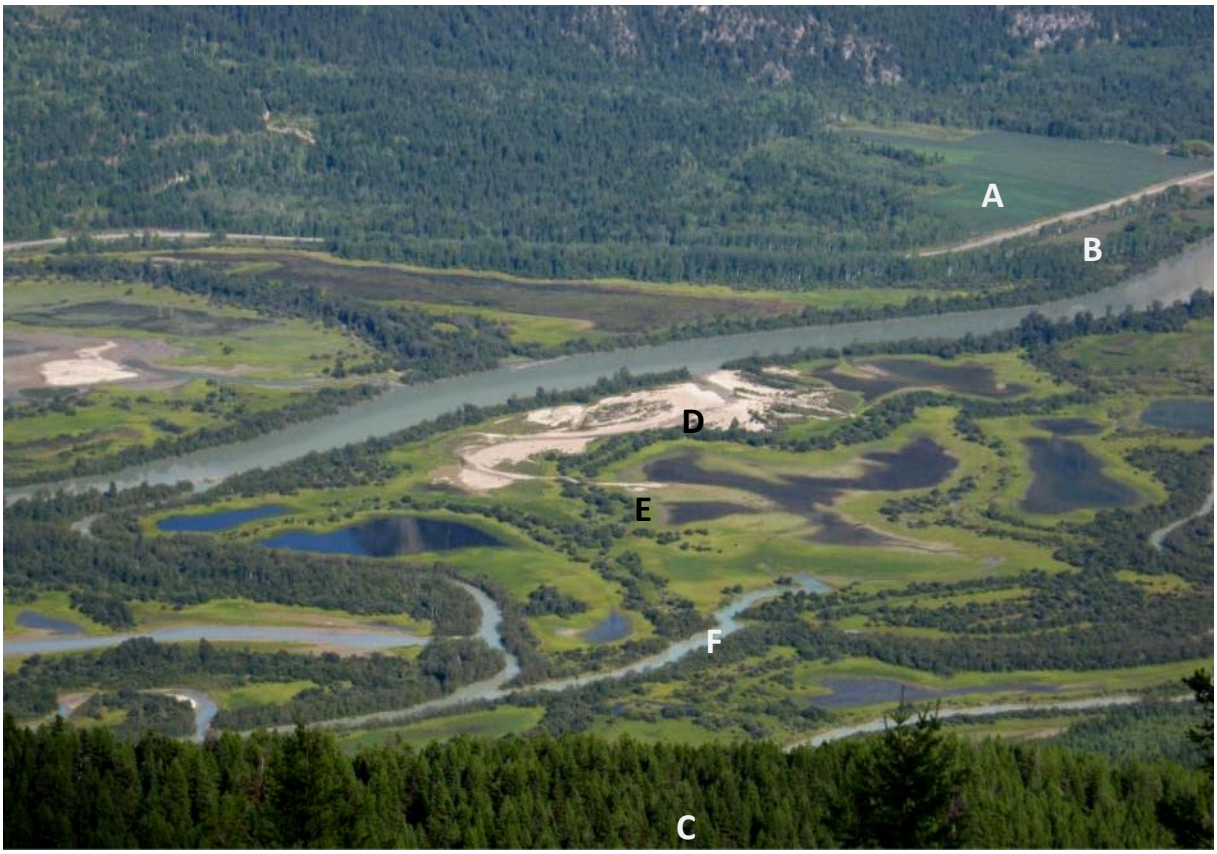

Figure 7. Overview picture of a part of the upper highly anastomosing reach, between Spillimacheen and Harrogate, August 2010. Flow is to the left (north). Locations A to F are described in the text.

4.1.1 Channels

In the upper anastomosing reach, three to five parallel interconnected channels are active on the floodplain. These channels have significant discharge, but always one channel accounts for the largest part of the discharge, this channel is called the main channel. The smaller secondary channels are often blocked by beaver dams and log jams. Residual channels in this area are divided based on two styles of infilling. The channel infilling can be dominated by lateral accretion of the levees (Figure 8A) or by vertical channel bed accretion (Figure 8B). Borings in those channels point out that there is also a difference in sedimentary fill. Channels filled in by lateral accretion consist of fine sediment (clay, silty clay and loam), while channels filled in by vertical bed accretion have a sandy fill. Spiral flow affects the infilling of upper Columbia River channels, causing inner bend residual channels to fill in vertically and outer bend residual channels to fill in with silt and clay. This is in consensus with the observations of Makaske et al. (2002) and the predictions of Kleinhans et al. (2008), see De Haas (2010) for evaluation of this spiral flow effect.

Figure 8. A: Lateral accretion of the levees. The mature trees from the levees invade the channel, making the channel narrower. B: Vertical channel bed accretion: Side bars invading channel 4 near Harrogate. Low pioneer vegetation covers the side bars, while mature trees dominate behind on the older levees. View is looking downstream from the studied transect.

4.1.2 Crevasse splays

Sandy crevasse splays are deposited in the floodbasin when overbank flow cuts a small channel (crevasse) through a levee, then transports and deposits sediment as a lobate sheet of sand and silt (splay) into the floodbasin (Figure 9A). As the splay develops, it progrades into the floodbasin. When crevasse channels incise through the splay deposits into the subsurface, a substantial portion of the flow can be taken over from the existing channels. This process can form a new channel belt in the anastomosing river system. The crevasse splay may cover or cross morphological elements in the floodplain, such as residual channels (Figure 9B). When a crevasse splay is not active anymore, it can become vegetated.

Figure 9. A: Crevasse splay formed after a levee break. The splay is located between Spillimacheen and Harrogate and is the same as visible on Figure 7 (D). B: Crevasse splay (foreground) crossing a residual channel (background). The residual channel vertically fills with wash load trapped by vegetation. This is the same splay as A and visible on Figure 7 (E).

4.1.3 Natural levees

The natural levees flank the channels and they consist of fine sand and loam, which fine and taper out in floodbasin deposits (clay) further away from the channel. The levees are densely vegetated with shrubs and trees. The levees can be up to one to two meter higher than the surrounding floodbasins.

4.1.4 Floodbasins

Floodbasins are wetland environments, which are the lowest parts of the floodplain (Figure 10A). During floods, floodbasins can receive floodwater with suspended load. Not all floodbasins drain seasonally and thus can maintain a dense aquatic flora. Therefore, floodbasin deposits are mixtures of clastic sediment (silty clay and clay deposits) and organic black-coloured mud. Those deposits are often bioturbated and sometimes laminated (Figure 10B). There is not much peat formation, because of high sediment input. The floodbasins are mainly vegetated with *Equisetum* and sedges.

Figure 10. A: Floodbasin partly filled with water. This floodbasin is located just downstream of the elevated cross-valley road at Spillimacheen. B: Thinly laminated organic and clastic mud. Core is taken with a gouge at boring 044 in the transect at Parson.

4.2 Proportions of sedimentary environments derived from aerial photographs

In this section the trends in the morphological variations on the aerial photographs are given. On 20 locations in the area between the Spillimacheen River and 10 km downstream of Parson, the width of all sedimentary environments (floodbasin, channel, crevasse and levees) perpendicular to the flow direction is measured. Figure 11 gives the results of those measurements. Figure 11A displays the width of the four sedimentary environments against the distance along the river. Figure 11B displays the proportions of the classes cumulative. The floodbasin environments are removed from this graph; those will make the proportions to 100%.

From this figure, no visible trend occurs in downstream direction for the channel environments. The width and proportions of the levee deposits and crevasse splay deposits show a decrease in downstream direction. This trend could be expected from the hypotheses about downstream fining and a decrease in bed-material load in the lower anastomosing reach. The total cumulative width of graph A shows a decrease in downstream direction, which indicates a decrease in floodplain width in downstream direction. On locations were an alluvial fan enters the valley, this causes a decrease in total amount of

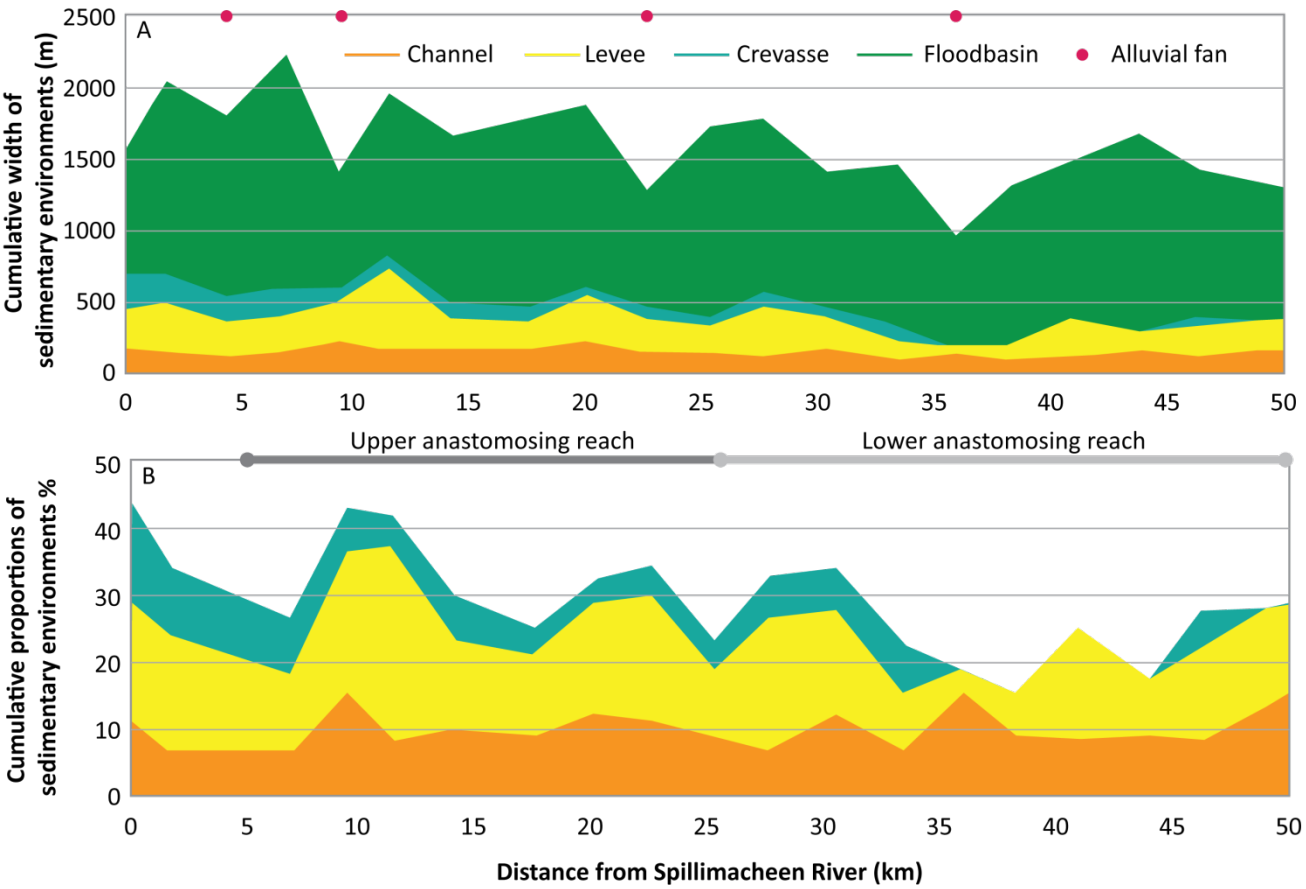

Figure 11. A: The cumulative width of all sedimentary environments plotted against the distance from the Spillimacheen River. Total cumulative width is equal to the floodplain width. The upper anastomosing reach starts at 5 km and the lower anastomosing reach at 26 km. Red dots displays the location of an alluvial fan at a measurement location. B: As A, but the values are given in cumulative proportions and are displayed without floodbasin deposits.

floodbasin deposits. The alluvial fans affect the channel, levee and crevasse splay proportions in less extent, because the fans are too small to influence the river pattern.

From the measurements on the aerial photographs, the floodplain width is measured and the number of channels is also counted. Those are plotted in a graph together to analyze the trend between the floodplain width and number of channels in downstream direction (Figure 12). Figure 12A is the natural situation. The maximum amount of channels in the highly anastomosing reach is 5 and on those places, the floodplain width is also relatively large. At the start of the upper anastomosing reach, 5 km from the Spillimacheen River, an increase in number of channels and an increase in floodplain width are visible. A factor that determines the floodplain width is the occurrence of alluvial fans in the floodplain. On locations with alluvial fans, the floodplain is narrower and has fewer channels, because of the restricted width. This is a temporary disturbance and does not show a general trend in downstream direction. Therefore, in Figure 12B the places where the floodplain is narrower due to an alluvial fan are corrected with an interpolated width from the measurement locations just up and downstream of the alluvial fan, so that the downstream trend becomes clearer. Both number of channels and floodplain width show a decreasing trend in downstream direction. This can be an indication that the degree of anastomosis is also

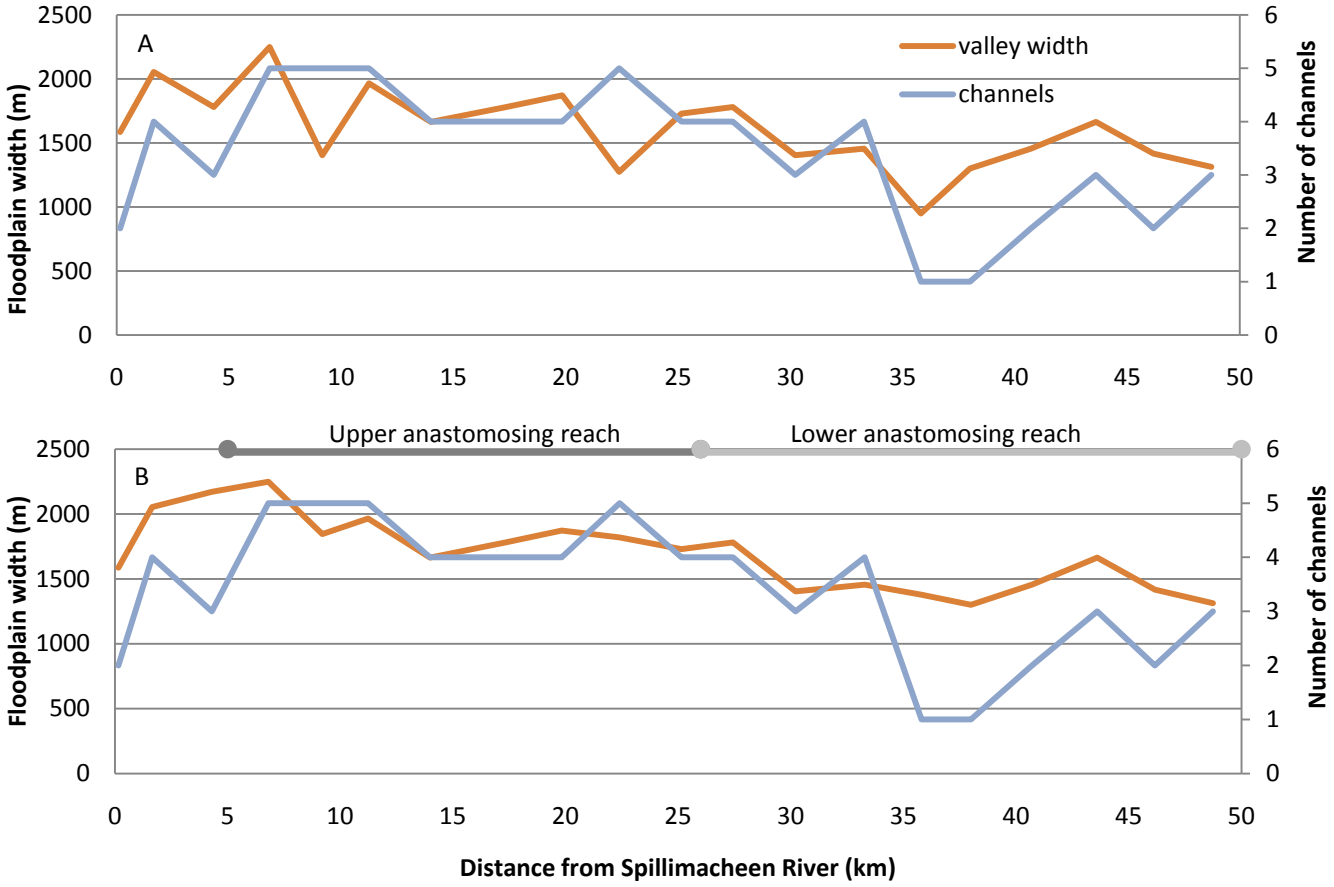

Figure 12. A: Floodplain width and number of channels plotted against the distance from the Spillimacheen River. Upper anastomosing reach starts at 5 km, lower anastomosing reach at 26 km. B: As A, but the width of locations near an alluvial fan are corrected, whereby the floodplain width at those spots is the width it would have without the alluvial fan.

a function of floodplain width. So, where the floodplain is wider, the number of channels can increase, because there is space for avulsions. In the Columbia Valley, the floodplain width is primarily restricted by mountain ranges on both sides. This causes that the decrease in floodplain width and number of channels is not necessary the result of sedimentary driving processes, but is also caused by the morphological setting which restricts the system.

4.3 Lithological borehole cross-sections and their genetic interpretation

In this thesis, the fieldwork results of Makaske et al. (2002) and new fieldwork results are combined. The lithological borehole cross-sections of the transects of Harrogate and Parson are plotted in one figure together with the transect near Castledale of Makaske et al. (2002) (Appendix 4). For the description of the borehole cross-section of Castledale, see Makaske et al. (2002). The lithological borehole cross-sections of Harrogate and Parson are described below together with the genetic interpretations of the borehole cross-sections (Appendix 5, Appendix 6).

4.3.1 Harrogate

Surface

In the transect near Harrogate five upper Columbia River channels are active during high water (channel 1, 3, 4, 5 and 7) and two residual channels are located on the floodplain (channel 2 and 6) (Appendix 2, Appendix 4). Channel 3 and 7 are the largest channels. No discharge measurements were made during the fieldwork, so it is not clear which channel caries most water discharge. But this is presumable channel 3, because of its size. Channel 1 is a small channel with beaver dams just downstream of the transect. On the line of the transect it is a channel with poorly developed levees making it plausible that it is a young channel. 20 m Upstream of the transect residual channel 2 branches off. Further upstream, channel 1 has better developed levees and likely was the upper course of channel 2 before the course of channel 1 in the transect was formed. Channel 2 is almost completely filled in and does not carry any water discharge. Channel 3 is partly blocked by a log jam, which is caused by poles placed in the bifurcation just upstream of the transect line (Figure 13). Those poles are placed by humans, to control the water flow direction of the upper Columbia River. Humans tried to force the main discharge through channel 4, to maintain a deep channel. This control was needed to have a deep enough channel for the steamboat, which navigated through the river 150 years ago. Those poles are now capturing drift-wood from the river and thereby create log jams. Channel 3 is the main channel with well-developed levees. Channel 4 is a very shallow channel, which was almost dry during of the fieldwork (Figure 5B). This channel has a sandy fill and has well developed levees. Judging from the size of the channel, it is likely that channel 4 was the former main channel, which is confirmed by the stakes indicating that channel 4 was part of the steamboat route. Channel 5 is a very narrow channel with densely vegetated levees. The mouth of this channel is almost entirely blocked by a log jam (Figure 13), which probably causes the abandoning of this channel. Channel 6 is a crevasse channel, splitting off from channel 7. This crevasse channel follows the

Figure 13. Log jam created by poles capturing drift-wood. Left channel is Harrogate channel 5, the channel right is the channel which bifurcates just downstream of this position in channel 3 and 4 of the Harrogate transect. View looking upstream.

path of a leveed residual channel in the transect. Channel 7 is a medium-sized channel with developed levees. Between all the channels-levee complexes floodbasins are located.

Subsurface

Boring 001-003 (Appendix 4) ends in hard light-grey sticky material, which is very poorly sorted and consist of silts and very angular and gravely grains. This material is interpreted as non-fluvial material; these are likely colluvium or regolith deposits. Around channel 1 and 2, a loamy complex is found. This is interpreted as a large levee system. It is probably formed because of the short distance between the channels which causes merging of the separate levee systems. It is also possible that the formation of channel 1 and/or channel 2 was preceded by the formation of a crevasse splay of loamy deposits and that channel 1 and/or channel 2 are the final result after the deposition of that loamy body. At this location, below the loamy deposits, humic deposits are found, with loamy deposits below it. The origin of this deep loam layer is not clear. Therefore in version 1 of the genetic profile (Appendix 5) it is indicated as crevasse deposits and in version 2 (Appendix 6) it is taken with the floodbasin deposits. In the deeper subsurface between boring 008 and 012, loamy deposits are found, interpreted as a levee. There are also sandy deposits suggesting a buried channel fill (residual channel A) with levees. Channel 4 is almost entirely filled in with coarse sand (boring 010 and 011), with loam complexes on its sides, interpreted as levees. Those asymmetrical levees suggest different periods of channel activity. The deepest part of the sand body (residual channel B) originates from the oldest period of activity, which has formed the deepest east

levee. After reactivation, it is likely that the west levee of channel B has been eroded. During reactivation, a larger channel was formed, whereby the east and west levees that are present at a relative depth of 3.5 m were formed. After that a new reactivation formed the present channel 4 with the levees that are present at the surface. In the subsurface between boring 018-022 a sheet like sand body was found roughly between 1-3 m below the surface. this sand-sheet is interpreted as crevasse splay deposits, because there are no levees or visible residual channels found with the borings. It is likely that channel 5 originates from this crevasse splay. The most likely explanation is that the crevasse splay was formed after a levee break upstream of the bifurcation of channel 4 and 5, whereby channel 5 was formed by this levee break as a crevasse splay channel. After the crevasse splay activity, channel 5 developed into a normal channel. This idea is confirmed by the fact that there is a sand-sheet under both levees of channel 5. Unfortunately the lithological composition at greater depth is not known in this area, because the borings are shallow due to the sand which is difficult to penetrate with the gouge. It was not possible to use the vibracore here, because of the dense vegetation. Between channel 5 and 6 more sand-splays deposits are found in the subsurface, also indicated as crevasse splay deposits. It is possible that the sand in boring 022 is a channel fill whereby this channel system caused the proposed levee, although this does not explain the sand in boring 023. In the most eastern part of the transect, a large loamy and sandy complex was found at a depth of 5 meter. The origin of this complex is unclear. Therefore it is classified as crevasse splay deposit in version 1 of the genetic profile and as levee deposit in version 2 of the genetic profile. Boring 028 and 029 end in sand which is likely alluvial fan material coming from the sides of the valley, because it is grayer and sorted worse than the channel and crevasse sand. On the sides of the floodplain were some peat complexes found. This peat is most often mixed with sediment and is therefore classified as humic clay. The peat complexes mainly exist of sedge-peat, peat with wood is only found in boring 003, 008 and 029.

4.3.2 Parson

Surface

In the transect of Parson two upper Columbia River channels are active during high water (channel 1 and 4) and two residual channels are located on the floodplain (channel 2 and 3) (Appendix 3, Appendix 4). Channel 4 is the main channel. Channel 1 splits off from channel 4, 1.5 km upstream of the transect. It is a channel with well-developed levees. Channel 2 is a residual channel which was connected to channel 1, but is now cut off by a crevasse splay just downstream of the transect line. Channel 3 is a residual channel with stagnant water during the fieldwork period. This channel is blocked by several beaver dams and splits of from channel 4. This channel has well-developed levees, and seems to have been a relative large channel formerly.

Subsurface

The first four borings on the west side of the transect (boring 036-039) end in very poorly sorted material which consist of silts and very angular and gravely grains, interpreted as colluvium or regolith deposits. Those non-fluvial deposits are covered with humic material with sedge remnants and channel deposits from channel 1. Approximately 2 m thick loamy deposits flank channel 1 on both sides, which are the levees of this channel. The tops of boring 040, 057 and 041 are very loamy and the floodplain is vegetated with shrubs at this position and some small residual channels are visible in the field. This irregular area is interpreted as a crevasse splay. Boring 040 and 057 end in sandy deposits. This sand represents a buried channel-fill with associated loamy levee deposits (residual channel A). Channel 2 is a small channel. The occurrence of the associated channel deposits is unknown. A loamy body is located by boring 042 and 043 at a relative depth of 6-7 m. The origin of this loam is not clear. Therefore in version 1 of the genetic profile (Appendix 5) it is indicated as crevasse deposits and in version 2 (Appendix 6) it is taken with the floodbasin deposits. With boring 038-044 a relatively wide spread humic layer was found at a depth of 2-4 m. This layer consist of thinly laminated organic and clastic mud with sedge remnants (Figure 10B) and is taken by the floodbasin deposits in the genetic interpretation. Borings 045-050 and 058 show a large sand body indicating a complex channel system. Whereby boring 058 is made on a beaver dam, just upstream of the transect and shows the channel-fill. On the west side of this system, loamy deposits are found at a depth of 4-8 m below the surface, which are the levees belonging to a former stage of channel 3. The east levee is probably eroded by residual channel B. After the activity of the channel B, channel 3 is reactivated whereby the present situation is formed. So, at this place on the transect at least four different periods of activity for this channel system were present. First, channel 3 was active, thereafter channel B eroded parts of the deposits from the older overbank deposits. After that, channel 3 was reactivated and now is abandoned. Boring 051-053 show a 70 cm thick humic clay layer. Around channel 4, the loamy deposits are much thicker on the west side than on the east side. The deeper loamy wedge in boring 053 may represent a crevasse splay cut by channel 4. Thereafter channel 4 has formed levees on both sides. Therefore, in the genetic profiles, the loamy deposits of boring 053 are split up into levee deposits and crevasse splay deposits. The floodbasin on the east side of channel 4 consist of peat, humic clay and clay, whereby the organics in the peat consist of sedge and *Equisetum*. Borings 054-056 ends in sticky light grey clay indicated as alluvial fan deposits, which are covered with humic material.

Remarks

By using only the gouge for the borings, the borings where sometimes shallow due to sand in the subsurface. Unfortunately, the vibracore was not always a good alternative for the gouge. The borings with the vibracore (010 and 011 in the transect of Harrogate) had very poor recovery, although a depth of 6 meters was reached. This was caused by the coarse sand and gravel in the channel-fill, which did not stay on place in the pipe. Other disadvantages of the vibracore are its weight and the length of the pipes, making it hard to handle with two persons.

Some places in the field were not accessible in the period of the fieldwork, because of water in the floodbasin. A solution could be to carry out fieldwork later in the year, but then the river stage would also be lower, so that not every location could be reached by a boat anymore.

4.3.3 Proportions of interpreted sedimentary facies derived from genetic profiles

The two versions of the genetic interpretation profiles are used to determine the mutual proportions of the four interpreted sedimentary facies: floodbasin deposits, levee deposits, channel deposits and crevasse splay deposits. Those results are described here.

In Figure 14A the total amount of the four classes of sedimentary facies is displayed by their proportions for the two versions of the genetic profiles. Hereby, a correction is applied for the large sand body in borings 047-050 in the profile of Parson. It is corrected to a more realistic width, because the plotted width in the genetic profiles is unrealistic. In Figure 14B the same graph is plotted as in Figure 14A, but there the floodbasin deposits are removed, to optimize the visibility of the differences between the other classes. From this, it becomes clear that the proportions of crevasse splay deposits decreases in downstream direction and the amount of floodbasin deposits increases in downstream direction. The trend in levee deposits is less obvious, because there is an increase in amount of levee deposits from Harrogate to Castledale and a decrease to Parson. The channel deposits show some increase in downstream direction.

The differences of the proportions of the interpreted facies between the two versions of the genetic profiles are not large. The difference is the largest in the amount of crevasse splay deposits. This was expected, because the interpretation of crevasse splay deposits were most uncertain during making the

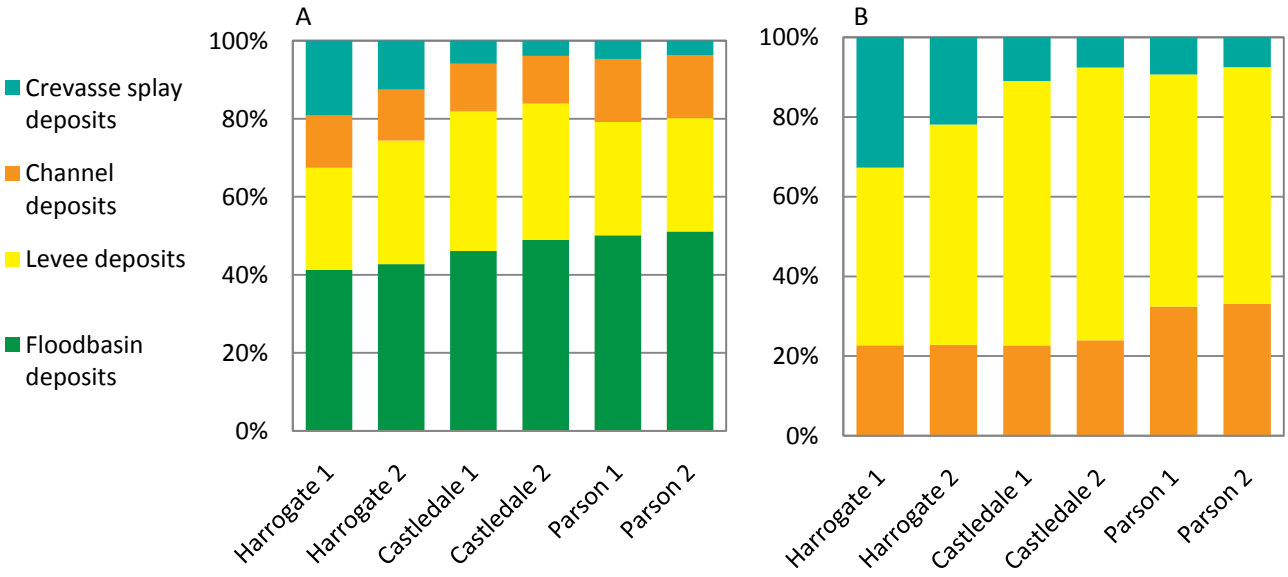

Figure 14. A: Proportions of all interpreted sedimentary facies classes displayed for the three locations of the profiles for two different versions of the genetic profiles, 1 indicates version 1, 2 indicates version 2 of the genetic profiles. B: As A, but without floodbasin deposits.

genetic interpretation profiles. The trends in deposition are the same in the two versions of the genetic profiles. Therefore, from now on, the mean of the two versions will be used in the further research on sediment budgets. This mean of deposits is displayed in Figure 15.

The proportions of the areas of the different interpreted sedimentary facies classes are used to create Figure 16. Here the change in proportions of all classes relative to the profile of Harrogate can be seen:

$$Proportion\ change = \frac{V_{C\ or\ P} - V_H}{V_H} * 100\% \qquad (15)$$

wherein $V_{C\ or\ P}$ is the proportion of a sedimentary facies for Castledale or Parson and V_H is the proportion of a sedimentary facies for Harrogate. From this, it becomes clear that floodbasin deposits and levee deposits increase in downstream direction. The change in channel deposits is less clear, from Harrogate to Castledale there is a decrease in area of channel deposits, while there is an increase in channel deposits from Castledale to Parson. The clearest trend is visible in the crevasse splay deposits; those deposits show a drop of 69% from Harrogate to Castledale and a drop of 73% from Harrogate to Parson (Figure 16).

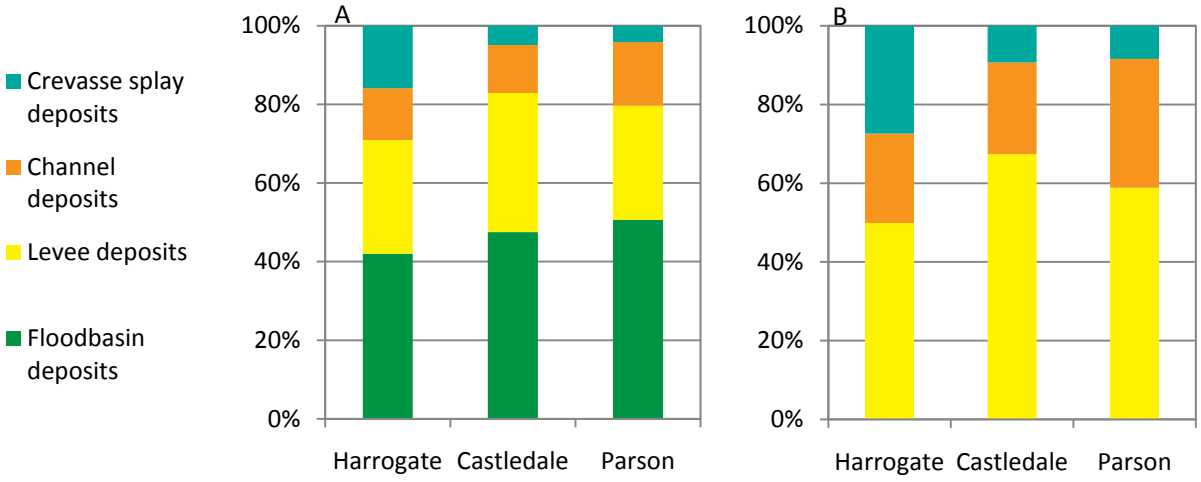

Figure 15. A: Proportions of all interpreted sedimentary facies classes displayed for the three locations of the profiles for the mean value of the two different versions of the genetic profiles. B: As A, but without floodbasin deposits.

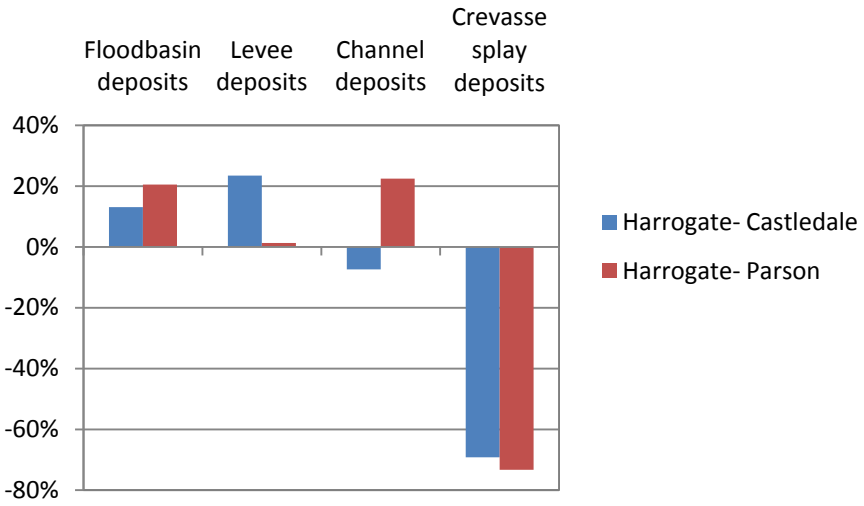

Figure 16. Differences between the interpreted sedimentary facies classes in proportions of Castledale and Parson relative to the profile of Harrogate. The areas of the different classes are taken as averages of the two different versions of the genetic profiles.

From the hypothesis of excessive sediment supply as driving mechanism in the anastomosing system, it is expected that the deposition of bed-material load (channel deposits and crevasse splay deposits) will decrease if the degree of anastomosis is decreasing. The degree of anastomosis is decreasing in downstream direction, so it is expected that the amount of channel deposits and crevasse deposits will decrease in downstream direction. This is the case for crevasse splay deposits but this is not the case for channel deposits. This is probably the result of an overestimation of channel deposits caused by a transect line which is not perpendicular to the channel body. When the channel body is obliquely cut, this will lead to a larger surface area.

4.4 Sediment deposition comparison between the genetic profiles and the aerial photographs

In this section the differences between classifying floodbasin, levee, channel and crevasse splay deposits with the genetic profile and the aerial photographs are investigated. This is done by plotting the top view of the three transects in three ways: 1) the top view of the aerial photograph measured along a straight line perpendicular to the floodplain; 2) the top view of the aerial photograph measured along the borehole transect line and 3) the top view of the genetic interpretation profile (Figure 17). This first way is the same as described in section 4.2. But it appears that this top view was different than the top view of the genetic profile, because the floodplain width differs enormously for those two. This is because the floodplain width of the genetic profiles is not the real floodplain width, but a projected line between the boreholes and the aerial photograph method does not follow the borehole locations exactly. Therefore, the morphological classification of the aerial photograph is also made on a line following the borehole locations exact as possible (top view 2). In Figure 18, the total proportions of those top views are displayed.

From Figure 17 and Figure 18 it becomes clear that the division of the morphological classes is different for the aerial photograph method and the genetic profile method. Therefore, the downstream trend in sedimentary classes also differs for the two methods. The differences are the largest between the first (aerial photograph with a straight line) and the third (genetic profile) method. Reason for this is that the locations of the measurements for those two methods are not exactly the same. However, the trends in changes of proportion of the morphological classes in downstream direction are expected to be the same. This is not the case; this can be explained by the inaccuracy of both methods.

First, when the transect line is not perpendicular to a morphological element, the measured surface of the element is not the real surface. This can lead to a wrong proportion of the measured surfaces of the different genetic classes. This can also explain unexpected results in proportions as with the increase of channel depositions by the transect of Parson, there: large sand bodies are drawn in borings 047-050 and

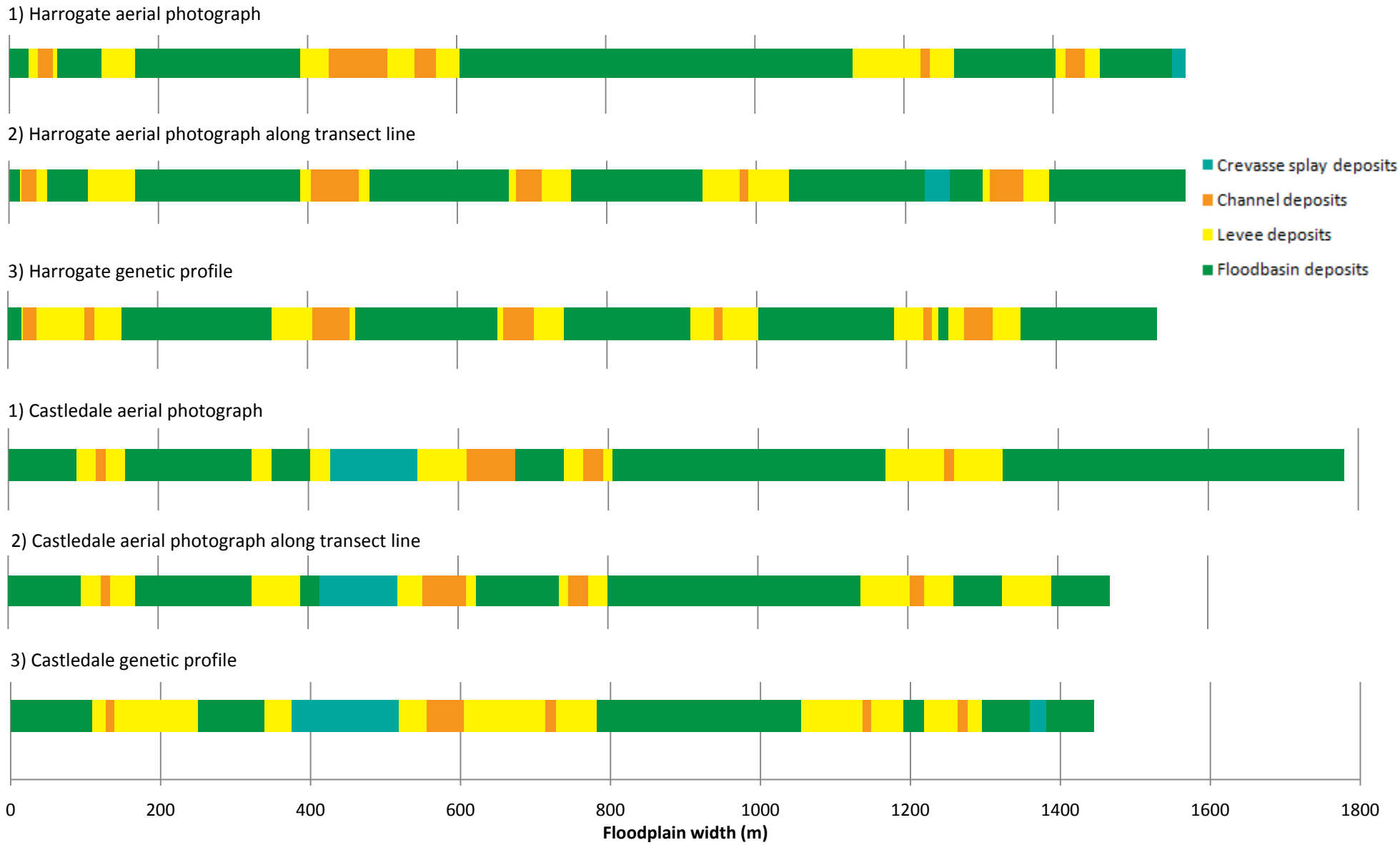

Figure 17. Top view of the aerial photograph interpretation along a straight line over the floodplain (1), along the transect line (2) and the top view of the genetic profiles (3).

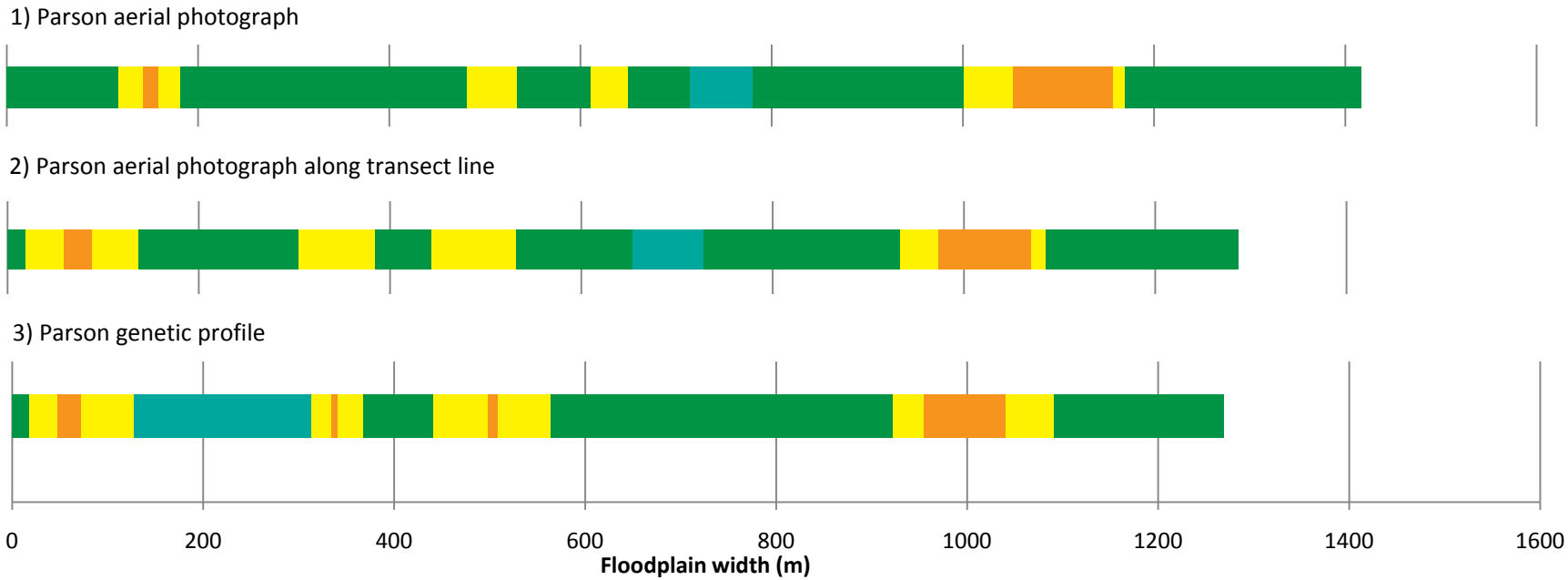

Figure 17.Continued.

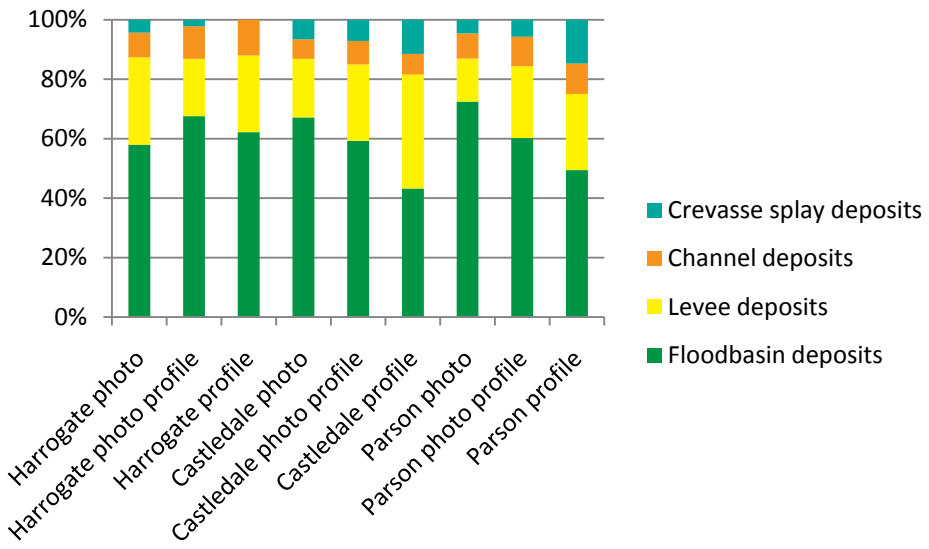

Figure 18. Proportions of all morphological classes displayed for the three locations of the profiles for the top view of the aerial photograph (photo), the top view of the aerial photograph along the transect of the genetic profile (photo profile) and for the top view of the mean genetic profile (profile).

in channel 4. The surface of the sand body in borings 047-050 is already corrected to a more realistic width, because the plotted width in the genetic profile is unrealistic. The top view of the aerial photograph which follows the borehole line gives about the same result as the genetic profile, because those methods cut the morphological elements in the same way.

Secondly, there are differences in classification of the morphological elements for the aerial photographs and the genetic profiles. This can explain the differences between the genetic profile top view and the aerial photograph which follows the borehole line. Levee deposits seem to be underestimated in both top views of the aerial photographs. This is because the only way to separate floodbasins from levees and crevasse splay deposits on an aerial photograph is on the basis of vegetation. Locations with trees and shrubs are interpreted as levee or crevasse splay deposits. This classification is based on observations from the field. But on places where the groundwater is too high for trees and shrubs, the deposits are possibly interpreted as floodbasins in the aerial photographs, whereas they should be interpreted as levee or crevasse splay deposits on basis of the sediment. Also, the genetic profiles seem to underestimate floodbasin deposits. This is visible in Figure 18, where the proportions of floodbasin deposits are much lower for the genetic profile versions of the top view than for the aerial photograph version for the transects of Castledale and Parson. During drawing the profiles, every lithological element different than floodbasin deposits was noted and possibly interpreted as another kind of deposit, while in the aerial photograph, only very clear structures were taken as separate classes.

What can be concluded from this comparison is:

- Differences between of the top view of genetic profiles and aerial photographs can be the result of oblique cutting of morphological elements and of wrong interpretation of the morphological elements.
- The aerial photograph of an area can lead to an underestimation of the classification of the deposits other than floodbasin deposits compared with the genetic profiles, while the genetic profiles of an area can lead to an overestimation of the classification of the deposits other than floodbasin deposits compared with the aerial photograph interpretation.

4.5 Channel chronology

By means of the cross-sections two graphs are made of the depths of the top of channel sand bodies and the base of the levees for the three transects, in order to analyze periods with channel activity (Figure 19). For the graph of the top channel sand bodies (Figure 19A), the channels with a clear reactivation phase, whereby a stacked channel in a former sand body is formed, are plotted as new channels. This is done for channel 3 and 4 of the transect near Harrogate and for channel 3 of the transect of Parson. For the transect near Castledale, the top of the sand bodies of the channels which are indicated by Makaske et al. (2002) are used. For the graph of the levee bases (Figure 19B) there are also some different active phases for one channel observed, recognizable by levees at multiple depths attached to one channel sand body; those levees are taken as a separate levee base. This is done for channel 3 of the Harrogate transect, for channel 3, 5 and A of the Castledale transect and for channel 3 of the Parson transect. Not all levees are plotted in this graph, because the base of deep levees is not always reached with the borings. It is also possible that some levees and channel sand bodies are missed by the borings. So, the deeper parts of the graphs are less reliable than the upper parts of the graphs.

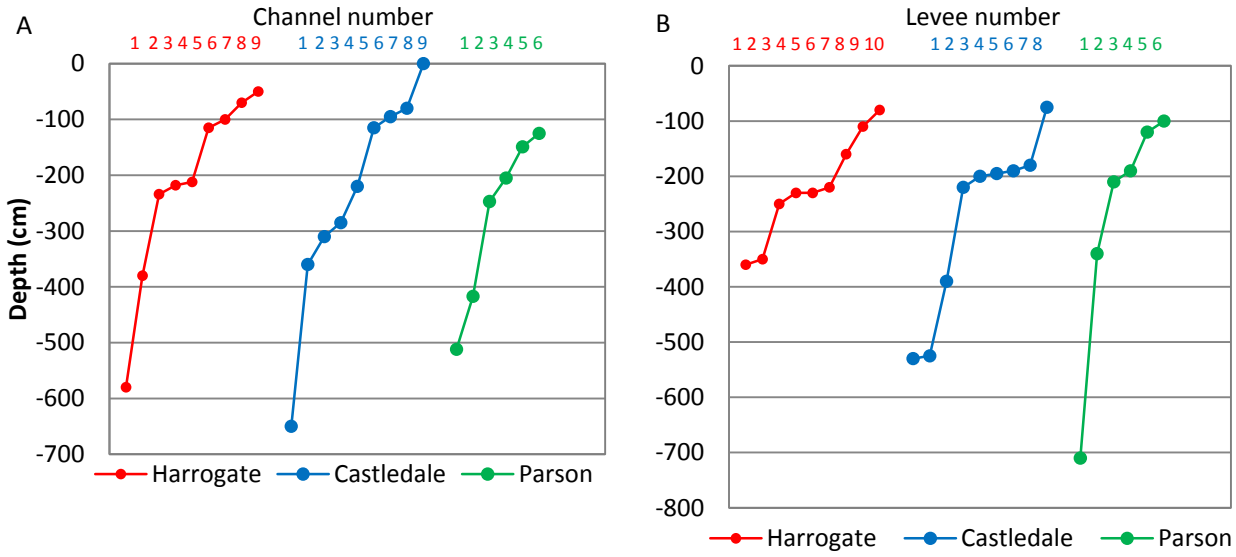

Figure 19. A: Sorted depth of the top of the channel sand bodies below an arbitrary datum near the floodplain surface. Channel number is determined by channel depth (1 for the deepest channel). B: As A, but this plot shows the base of levee deposits.

The channel sand body depths are not equally spaced in the cross-sections. The channel sand bodies in the transect near Harrogate show a group of channel bodies near -200 cm below the arbitrary date and a group of channel bodies at a depth of -100 cm. The channels in the cross section of Castledale are somewhat more evenly distributed in depth, but cluster around -300 cm and near -100 cm below the arbitrary date. For the transect of Parson, no clear clustering is visible, because of the fewer channels in this transect and because of a more even distribution of the channel sand bodies in depth. The bases of the levees are also not equally spaced in the cross-sections. The levees in the transect near Harrogate show a group of levees near -350 cm and a group at a depth of -250 cm. The bases of the levees in the cross-section of Castledale are clustered around a depth of -520 cm and -200 cm. For the transect of Parson, also no clear clustering is visible.

Both methods show clusters in the channel chronology. Those different clusters are an indication for a depositional variability over time. The clustering of channel sand bodies and levees in depth is most clear for the transects of Harrogate and Castledale. This clustering indicates perhaps periods with more and less channel activity. In between those periods with a cluster of channel sand bodies and levees, probably a less anastomosing river system appears.

Both methods appear to be useful in displaying channel chronology. An advantage of the channel sand body analysis is that more information is gained about the deeper parts of the cross-sections, than for the levee bases. Because in these cross-sections, not all levee bases are reached with the borings, therefore Figure 19B gives a poor impression of the channel chronology at greater depths. A disadvantage of the channel sand body analysis is that the top of a sand body displays the end phase of channel activity. This end phase is not always exactly displayed with the top of the sand body, because a channel can also fill in with clay, loam or organics. The levee base analysis is therefore a better measure for the channel chronology, because it displays the beginning of sedimentation of a channel.

4.6 AMS radiocarbon dates

Table 2 displays the results of the AMS radiocarbon dating of the macrofossils presented in Table 1. From those ages, the sedimentation rates are be calculated. In Figure 20, a time depth diagram of the radiocarbon dates of Harrogate, Castledale and Parson are plotted. The mean sedimentation rate for Harrogate is 1.66 mm/yr. Sample 2.2A is hereby rejected. This sample diverges from the other samples probably because of peat compaction; this sample is located on top of a peat layer, which makes compaction plausible. Compaction can also have had a role by Castledale sample 3A, 3B and 3C, because those dates also differ from the other samples in the age series. Makaske et al. (2002) calculated an average long-term floodplain sedimentation rate of 1.75 mm/yr for Castledale. This is higher than the average long-term floodplain sedimentation rate of Harrogate. However, it was hypothesized that the sedimentation rate would decrease in downstream direction. But Harrogate is located upstream from Castledale and it is therefore expected to have a higher sedimentation rate than Castledale. By

Table 2. AMS radiocarbon age determinations and calibrated ages from floodplain material of the cross-sections of Harrogate and Parson. Calibrated with the Groningen calibration program (version CAL25) (Van der Plicht, 1993) with BP is before 2009. Minimum sedimentation rate is based on minimum depth and maximum age, median sedimentation rate is based on average depth and median age, maximum sedimentation rate is based on maximum depth and minimum age.

Location	Sample	Laboratory no. (GrA)	Depth below surface (cm)	^{14}C age (^{14}C yrs BP)	Median age (cal. yrs BP)	2σ age (cal. yrs BP)	Min. sedi. rate (mm/yr)	Median sedi. rate (mm/yr)	Max. sedi. rate (mm/yr)
Harrogate	2.2A	46792	421-423	675 ± 45	700	759-639	5.55	6.03	6.62
Harrogate	2.7C	46797	644-646	3655 ± 65	4046	4079-3819	1.58	1.59	1.69
Harrogate	2.8B	46795	670.5-673	3575 ± 70	3937	4119-3739	1.63	1.71	1.80
Harrogate	2.8A	46793	668.5-670.5	3590 ± 45	3956	3961-3849	1.69	1.69	1.74
Parson	2.12E	46800	554-556	3475 ± 55	3808	3939-3659	1.41	1.46	1.52
Parson	2.12D	46566	552-554	3545 ± 45	3897	3999-3759	1.47	1.42	1.39
Parson	2.14D	45815	522-524	3635 ± 40	4016	4119-3899	1.27	1.30	1.34

analyzing the radiocarbon dates of Castledale of Makaske et al. (2002) it shows that the samples 3A, 3B and 3C are causing this high sedimentation rate. It is possible that sample 3 is located on the top of an underlying peat layer, while the other samples (except 2.2A) are located on the bottom of a peat layer and thus less vulnerable for compaction. When sample 3 is rejected, the average long-term floodplain sedimentation rate of Castledale becomes 1.53 mm/yr. The mean sedimentation rate near Parson is 1.39 mm/yr. So, the sedimentation rate near Harrogate is significantly higher than near Parson, because the ranges of the sedimentation rate from minimum to maximum do not overlap for Harrogate and Parson. All dated material from Harrogate and Parson have an age of around 3900 yrs BP. Those radiocarbon dates indicate probably a period with a reduced activity of the upper Columbia River, whereby peat growth became possible. Because peat layers are not common in the upper Columbia River, due to the high amount of suspended load in the floodbasins. In conclusion, the average long term sedimentation rates derived from the AMS radiocarbon dates show a trend in downstream direction from 1.66 mm/yr near Harrogate, to 1.53 mm/yr near Castledale and to 1.39 mm/yr near Parson.

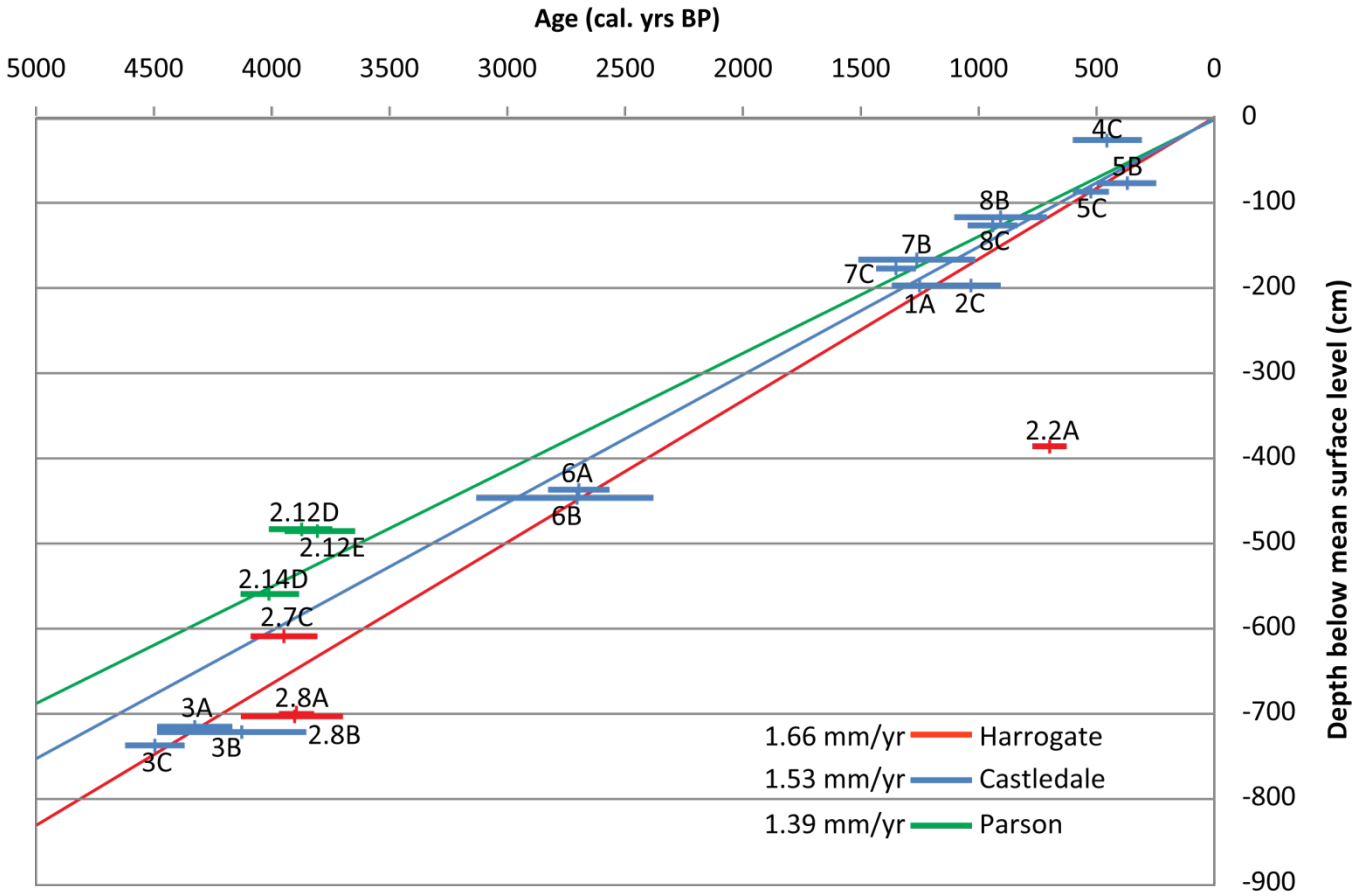

Figure 20. Time depth diagram with radiocarbon data from this study (Harrogate and Parson) and from Makaske et al. (2002) (Castledale). Calibrated age of ^{14}C dated samples is plotted against the mean depth of a sample relative to a depth based on the mean depth of the cross-section surfaces. Widths of the bars represent the 2σ error range of the calibrated age.

Remarks

The best locations for sampling organic samples for the AMS radiocarbon dating were along the sides of the floodplain. On those locations, the most peat growth took place. This can be explained by the channel activity in the floodplain. The largest channels are most of the time positioned in the center of the floodplain, therefore, floodbasins flanking those main channels receive most suspended load. The deposition of suspended load disturbs the peat growth. So, more organics can be found near the sides of the floodplain. Unfortunately, the average sedimentation rate is possibly lower on the sides, because those locations receive less sediment. And thus those locations are less accurate for the calculations of the average sedimentation rate, because the sedimentation rate can be lower than average. However, the cross-sections do not show more accumulation in the center of the floodplain, and therefore the dates of the organics from the sides of the floodplain will be used as an estimate for the average long term sedimentation rate.

4.7 Sediment dynamics

To test the idea that excessive sediment supply causes a higher aggradation rate in the upper anastomosing reach than in the lower anastomosing reach, three methods were used to get insight into the sediment dynamics; those are presented in Table 3:

1) Measured sediment transport values of Locking (1983) and sediment transport predictions of Makaske et al. (2009) were used to calculate the sedimentation rate, column 1 and 2 in Table 3.
2) Sediment transport predictors were used to calculate the sedimentation rate for the upper and the lower anastomosing reach, with two different bed load predictors and at two different locations, column 3 to 6 in Table 3.
3) The genetic interpretation of the borehole cross-sections were used to make an estimate of the sedimentation rate for the total area and separate for the upper and lower anastomosing reach, column 7 and 8 in Table 3. AMS radiocarbon dates are used to measure the sedimentation rate for the upper and the lower anastomosing reach on basis of the genetic interpretation profiles and are presented in column 9 in Table 3.

The sediment transport measurements of Locking (1983) are published as suspended load and as bed load. Here, that suspended load is taken as wash load, because Locking (1983) investigated that her suspended load concentration almost totally consisted of wash load. Bed load is taken as bed-material load, however, this does not include suspended bed-material load, which is partly measured in the suspended load concentration. Therefore the total amount of sediment load (wash load + bed-material load) is given to make comparison with other methods possible (column 1).

Table 3. Sediment budgets calculated with 1) sediment transport measurements of Locking (1983); 2) predictions from Makaske et al. (2009); 3) predictions with the Van Rijn (1984) bed load transport predictor at the location of the gauging station of Spillimacheen, the transect near Castledale and the gauging station of Nicholson (SCN); 4) predictions with the fitted bed load transport predictor at the locations SCN; 5) predictions with the Van Rijn (1984) bed load transport predictor at the location of the upstream gentle transect, steep reach transect and the gentle reach transect (USG); 6) predictions with the fitted bed load transport predictor at the locations USG; 7) mean sedimentation budgets derived from the genetic profiles of Harrogate and Parson; 8) sedimentation budgets derived from the genetic profiles of Harrogate (Upper Reach) and Parson (Lower Reach); 9) sedimentation budgets derived from calculated sedimentation rates based on ^{14}C ages. WL= Wash load, BL= Bed-material load.

		1) Measurments Locking (1983)		2) Predictions Makaske et al. (2009)		3) Predictions with Van Rijn (1984) SCN		4) Predictions with fitted SCN		5) Predictions with Van Rijn USG		6) Predictions with fitted USG		7) Estimate from Genetic profiles		8) Estimate from Genetic profiles		9) Calulated from ^{14}C dates	
		m^3/1000yr	mm/yr	m^3/1000yr	mm/yr	m^3/1000yr	mm/yr	m^3/1000yr	mm/yr	m^3/1000yr	mm/yr	m^3/1000yr	mm/yr	m^3/1000yr	mm/yr	m^3/1000yr	mm/yr	m^3/1000yr	mm/yr
Upper	WL															3.37E+07	1.72		
Reach	BL			2.57E+07	1.31	-4.20E+07	-2.15	-1.03E+07	-0.52	-1.48E+08	-7.55	-4.10E+07	-2.09			1.38E+07	0.70		
	Total															4.75E+07	2.43	3.26E+07	1.66
Lower	WL															6.87E+07	1.50		
Reach	BL			8.80E+06	0.19	3.19E+07	0.70	6.45E+06	0.14	1.41E+08	3.08	3.83E+07	0.84			1.75E+07	0.38		
	Total															8.62E+07	1.89	6.37E+07	1.39
Total	WL	2.56E+08	3.92											1.05E+08	1.61	1.02E+08	1.57		
Area	BL	5.42E+07	0.83	3.45E+07	0.53	-1.01E+07	-0.16	-3.83E+06	-0.06	-7.23E+06	-0.11	-2.66E+06	-0.04	3.55E+07	0.54	3.13E+07	0.48		
	Total	3.10E+08	4.75											1.41E+08	2.16	1.34E+08	2.05	9.63E+07	1.47

The combined measured bed load transport data from Locking (1983) and the calculated bed load transport data from the Castledale transect of Makaske et al. (2009) are given in column 2. These results are compared with sediment transport predictions carried out for the whole reach. These calculations are carried out in four different versions (column 3 to 6). To compare the bed load transport calculations directly with the calculations and measurements presented by Makaske et al. (2009), bed load transport is calculated at the same positions: the transect line of Castledale and the gauging stations of Locking (1983), near Spillimacheen and Nicholson. These calculations are called SCN and are made with the Van Rijn (1984) predictor (as Makaske et al., 2009) and with the fitted predictor of De Haas (2010) (column 3, 4). Column 5 and 6 gives the results of the bed load transport calculations at the upper gentle reach, the steep reach and the gentle reach are used (USG) using the Van Rijn (1984) predictor and the fitted predictor.

The sediment budgets derived from a mean deposition from the genetic profiles of Harrogate and Parson (column 7) gives comparable results with the sediment budgets from Locking (1983). In column 1 and 7, the largest part of the sedimentation consists of wash load (stored in floodbasins and levees). With the genetic profiles, the sedimentation rates for the upper and the lower anastomosing reach are also calculated separate (column 8). Those calculations show a higher deposition rate for wash load and bed-material load in the upper anastomosing reach than in the lower anastomosing reach. Wash load deposition is here also higher than the bed-material load deposition. The reason that the total sediment budgets calculations are different for column 7 and 8, is because the mean (column 7) is calculated with a mean of the Harrogate and Parson profile for the total area and not with a weighted mean. A weighted mean would take the differences in surface area of the upper and lower reach into account, but here it is chosen to take one mean for the total area.

With the average sedimentation rates derived from the AMS radiocarbon dating, the total amount of sedimentation is calculated (column 9). The sedimentation rate in the upper reach is higher than in the lower reach. The calculated total sedimentation budget is therefore higher in the upper reach than in the lower reach.

The total amount of bed load deposition calculated by Makaske et al. (2009) (column 2) with this method is comparable with the calculations of bed-material load with the genetic profiles. These are almost the same; this indicates that suspended bed-material load can be neglected in the bed-material load calculations.

The bed load transport rates are plotted in Figure 21A with arrows to compare the bed load transport calculations with the calculations of Makaske et al. (2009) and the calculations with the genetic profiles. The rates calculated during this research differ from data of Makaske et al. (2009). Measured input of Locking (1983) near Spillimacheen is much larger than the predicted input of this research. The output at

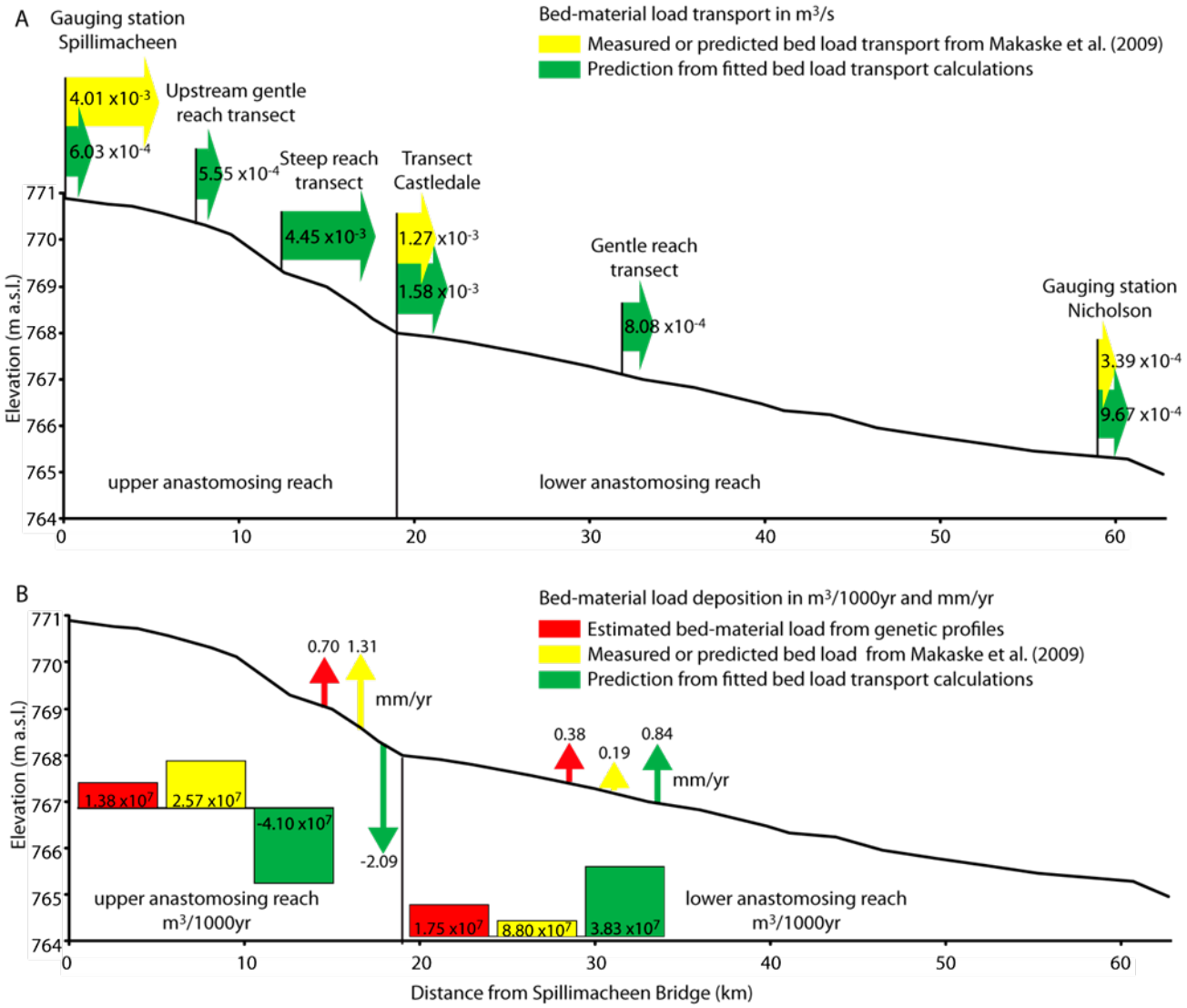

Figure 21. Longitudinal profile of the upper Columbia River main channel, showing the relatively steep upper reach and the relatively gentle lower reach. A: Bed-material load transport. Yellow and green arrows give the bed load transport at the gauging stations of Locking (1983) (Spillimacheen and Nicholson), at the transect of Castledale and at the upper gentle reach, the steep reach and the gentle reach calculated with the Van Rijn (1984) bed load predictor (yellow) and with the fitted bed load predictor (green). B: Bed-material load deposition. Red, yellow and green bars represent the deposition of the bed-material load in the upper and lower anastomosing reach. In red the prediction with the genetic profiles, in yellow the prediction of Makaske et al. (2009) and in green the bed load deposition calculated with the fitted bed load transport calculations, calculated for the floodplain transects at the upstream gentle reach, the steep reach and the gentle reach.

Castledale is larger for these predictions than for the predictions of Makaske et al. (2009). Near Nicholson, measured and predicted is almost the same. In between these locations, the bed load transport is calculated at the locations at the upper gentle reach, the steep reach and the gentle reach are used (USG), which shows the highest transport at the steep reach. For the calculation of the sedimentation budgets of Figure 21B, the bed load predictions at the locations USG are used with the fitted bed load predictions. For those calculations, it is assumed that the amount of suspended bed-material load can be neglected, and therefore the results of the bed load predictions results can be compared with the bed-material load results from the genetic profiles. The clearest result of the bed load predictions is that there is net erosion

instead of deposition in the upper anastomosing reach, whereas the estimates from the genetic profiles and the predictions of Makaske et al. (2009) give about the same amount of deposition. Deposition of bed-material load estimated with the genetic profiles is higher in the lower anastomosing reach than in the upper anastomosing reach. In the lower anastomosing reach, all three bed-material load deposition calculations are of the same magnitude, indicating deposition.

Remarks

The sediment budget estimations from the genetic profiles are not very accurate. At this moment, the total area of the genetic profiles is used as an estimate for the deposition in 3000 yr. This is a rough estimate, neglecting the effect of shallow borings and assuming a steady deposition over 3000 years. When more time was available, it would become possible to make budget calculations for different periods of deposition by making time lines in the transects. Thereafter, a correction for "lack of sediment" due to shallow borings can be made.

The bed load transport calculations are very sensitive for the slope of the location of the calculation. For these calculations the measured water surface profile slope of Abbado et al. (2005) is used, which gives only the slope of the main channel. This slope is taken to be representative for the whole floodplain width at the position of a measurement. At the steep reach with the hypothesized large deposition, the predicted bed load transport is large, due to this steep reach. Due to this large transport capacity, erosion is predicted in this reach rather than deposition (-2.09 mm/yr, Figure 12B). This does not mean that there is actually erosion, because when more sediment enters the reach than can be transported, deposition will take place. This is illustrated by the difference between the measured sediment input at Spillimacheen ($4.01 * 10^{-4}$ m^3/s, yellow arrow Figure 21A) and the predicted sediment transport capacity ($6.03 * 10^{-4}$ m^3/s, green arrow Figure 21A). This measured sediment input exceeds the predicted sediment transport capacity, what will cause deposition. Even if there is actual erosion, because the predicted sediment output near Castledale is larger than the input near Spillimacheen ($1.58 * 10^{-3}$ m^3/s against $6.03 * 10^{-4}$ m^3/s, green arrows Figure 21A), this will not mean that this is the case for a long time. Because, the genetic profiles show net accumulation, and sediment transport measurements and predictions are based on temporally river morphologies.

5 Discussion

The aim of this research was to contribute to the detailed understanding of the origin of anastomosis. The research was set up to test different theories of the origin of anastomosis. The present work aimed to investigate if excessive sediment supply is the driving force behind anastomosis. During this research different methods are used to get insight in the sediment dynamics of the anastomosing system of the upper Columbia River, but the methods give different results and are disputable. Section 5.1 discusses the reliability of the sediment budgets presented in this research. Section 5.2 compares the upper Columbia River to the Rhine catchment. Section 5.3 discusses the results concerning the sediment budget calculations and comparison with existing sedimentation calculations. Section 5.4 discusses the cause of anastomosis by discussing the tested hypotheses and the research questions.

5.1 Reliability of the calculated sediment budgets

Six methods are used to get insight in the sediment dynamics in the studied reach. Here, the methods will be discussed by using the genetic profiles, aerial photographs, radiocarbon dates and sediment transport predictions.

The sediment budget calculations with the genetic profiles are based on the methods presented by Erkens (2009) for the quantification of the sediment dynamics of the Rhine catchment. However, some debatable simplifications are used. The total area of the genetic profiles is used as an estimate for the deposition rate in 3000 yr. This is a rough estimate, whereby the effect of shallow borings is neglected and whereby a steady deposition over the 3000 years is presumed. To improve this estimate, the ^{14}C dates must be used to make time-lines in the profiles, whereby budget calculations for different periods of deposition can be made.

The use of aerial photographs in observing a trend in morphological elements is found to underestimate the deposits other than floodbasin deposits compared with the genetic profiles. The genetic profiles seem to overestimate the classification of the deposits other than floodbasin deposits compared with the aerial photographs. Both methods have errors because of oblique cutting of morphological elements and of wrong interpretation of the morphological elements. Therefore, they are not accurate enough to use alone for a budget investigation.

The sediment transport predictors are sensitive to the slope of the location of the calculation. For these calculations, the measured slope of the mean channel of Abbado et al. (2005) is used. This slope is possibly not representative for the whole floodplain width and for the total calculated period of 1000 years. These slope calculations can perhaps be improved by using available radar elevation measurements of the area. These represent channel and floodplain elevations, which can complement the elevation measurements of Abbado et al. (2005). This research and the research of Makaske et al. (2009) lean strongly on the division of the Columbia Valley into two sub-reaches. The boundaries of these sub-

reaches, with a steeper valley slope (upper anastomosing reach) and with a low valley slope (lower anastomosing reach), are based on the elevation measurement of Abbado et al. (2005). These measurements are based on a single time measurement. It would improve this research when these measurements would be verified.

The calculated average sedimentation rate is not representative for the whole floodplain. Makaske et al. (2009) found different sedimentation rates for levees and channel beds. For the upper anastomosing reach of the upper Columbia River, the bed aggradation rates in the main channel outpace levee accretion (Figure 22). For the lower anastomosing reach, main channel bed aggradation rates are lower. Channel shallowing is still likely to occur in this reach, but at an absolute slower rate than in the upper anastomosing reach, because the bed load input in this reach is much lower than in the upper reach (Makaske et al., 2009). It is possible to measure floodbasin sedimentation rate separate from the average sedimentation rate, however, this is only possible on places where no other deposits than floodbasin deposits are found in the dated core. Or where long intervals of floodbasin deposits are found sandwiched between dateable peat layers in one core. Those spots are rare, due to the high dynamics in the system and the scarcity of dateable organics. Measuring the levee sedimentation rate is only possible when there are organics just below the levees, but this is rare here. A way to overcome this problem is by using other dating techniques as optical stimulated luminescence dating; enabling dating of sandy deposits, but this requires specialized knowledge, which was not available during this research.

For an accurate age-depth control, the depth control of the samples must be very precise. But the leveling circumstances where not always ideal. Leveling is less accurate if the distances between the measuring points are large. This was unavoidable on places where the floodbasins were filled with water. Leveling is also less accurate if the level has to be moved frequently, this was often the case, because of densely

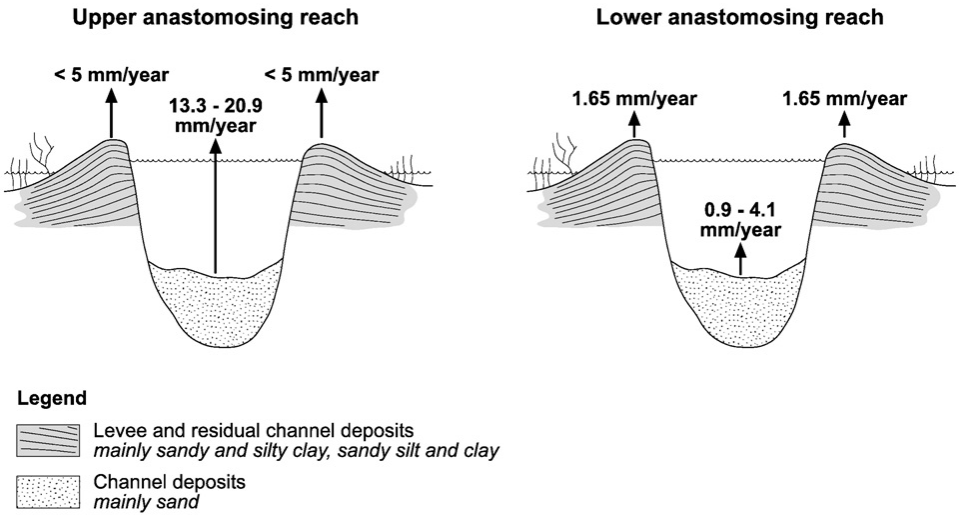

Figure 22. Bed and levee accretion rates for the upper Columbia River main channel in the upper and lower anastomosing reach. Vertical exaggeration approximately 10x (From: Makaske et al., 2009).

vegetated levees. But presumably leveling is a good estimate of the elevation because, potential measuring errors will become averaged over the transect.

Erkens (2009) analyzed trends in sediment deposition of suspended load and bed load. In the classification used by Frings et al. (2008); this would be called wash load and bed-material load. During this research, this classical classification is used. Erkens's (2009) suspended load consists of floodbasin deposits and overbank deposits (levee and crevasse splay deposits), while in this research, wash load consist of floodbasin deposits and levee deposits. Erkens's (2009) bed load consists of channel deposits, while here bed-material load consists of crevasse splay deposits and channel deposits. But in this research; almost no bed-material deposits were found in the levees and the major part of the crevasse splay deposits consists of bed-material load. Therefore, this classification is used, and not the one of Erkens (2009). Both classifications are a simplification of the real division of wash and bed-material load and are therefore disputable. But due to the used classification, the amount of wash load can be overestimated at locations where the levees are composed of bed-material load and the amount of bed-material load can be overestimated at locations were crevasse splay deposits are also composed of wash load.

5.2 Comparison with the Rhine catchment

Frings (2008) described downstream fining of the bed sediments in sand-bed rivers such as the river Rhine. During this research, sediments in the upstream and downstream parts of the upper Columbia River are investigated, wherefrom the grain-size distribution is investigated. From Frings (2008) it is hypothesized that selective transport and sediment addition or extraction causes downstream fining in the upper Columbia River. From the sediment budget calculations of the genetic profiles, a decreasing trend in the coarse bed-material load is discovered and an increasing trend in amount of fine wash load is discovered. This was also observed by Abbado et al. (2005). This research illustrates thereby the theory of Frings (2008) and thus, the upper Columbia River shows comparable processes as the river Rhine.

The geographic setting of the Columbia Valley shows many similarities with the north Upper Rhine Graben. This graben (valley) is located between Basel (Switzerland) and Mainz (Germany). This valley is a major sink for Rhine sediments and has a mountain-dominated discharge regime, comparable to the Columbia Valley. The Rhine in this valley was a multiple channel river during the Late Pleniglacial and Early Holocene. During the Middle Holocene, the system consisted of multiple shallow (<5 m) channels with a low sinuosity. Erkens (2009) explored the possibility that changes in fluvial style are caused by intrinsic response to local factors as an alternative for earlier presumed allogenic forcing. The valley slope of the northern Upper Rhine Graben is low, because of the presence of a local base level. Consequently, the stream power of the River Rhine is low, which hampered further incision as in the upper Columbia River. It requires more energy for an incised and straightened stretch of the river to become meandering again, as more material has to be removed. This implies that intrinsic response of the river to site-specific factors

(low gradient, incised valley) provides an explanation for the local trend of decreasing meander sinuosity. Increased suspended sediment delivery during the Late Holocene (an allogenic forcing) is likely to have caused a further increase of bank resistance and thereby amplified the existing trend. This situation is comparable with the upper Columbia River, but this theory contradicts the theory of excessive sediment supply (an allogenic forcing) as explanation for the multiple channel system. Because of the comparability of those two rivers, the given site-specific factors can be taken as part of the explanation of the anastomosis of the upper Columbia River. This explains also the limited scale of the anastomosis, because when localized site-specific factors as local differences in subsurface or gradient cause anastomosis, the extent will be limited.

So, this makes it plausible that the origin of anastomosis is not only a factor of excessive sediment load supply. When anastomosis is only driven by the input of sediment, anastomosing systems would probably be more common, because an overload of sediment can occur in many rivers. Anastomosis is also not only an intrinsic response to local factors, because then, no triggers for avulsions would be generated. In the upper Columbia River this trigger is most likely generated by the accumulation of bed-material load on the channel bed, leading to gradual decrease in flow capacity, increased overbank flooding and cutting of new channels on the floodplain. Although triggers for avulsions can also be generated by local factors such as log jams, ice dams, beaver dams and a decrease in bank resistance. So, the river setting with its own intrinsic factors can maintain an anastomosing system when allogenic forcing amplifies the trend of excessive sediment load supply.

5.3 Aggradation rate of the upper Columbia River

Makaske et al. (2009) used a non-uniform method to estimate the bed load deposition in the upper and lower anastomosing reaches: they used sediment transport measurements of Locking (1983) and sediment transport predictions. This lead to the conclusion that the bed load deposition is higher in the upper anastomosing reach than in the lower anastomosing reach. Makaske et al. (2009) used the sediment transport predictions as if those values represent the real sediment transport rates. But, the sediment transport predictions are only an indication of the sediment transport capacity. It is possible that real sediment transport is higher or lower than the transport capacity, which will affect the estimates of sediment deposition or erosion in the studied reach.

Using a non-uniform method to register trends in data will give errors. Makaske et al. (2009) used sediment transport measurements and sediment transport predictions, whereby errors arise by both methods. This effect especially plays an important role when analyzing the downstream trend in sediment transport, because the difference between upstream and downstream sediment transport is small, so that measurement errors can take a high proportion of the observed trend.

Therefore, during this research, sediment deposition is recalculated using only sediment transport predictors (a uniform method). The results of those calculations are different from the results of Makaske et al. (2009) and are in conflict with the hypothesis of excessive sediment input as driving force for the anastomosis of the upper Columbia River. At the steep reach with the hypothesized large deposition, the predicted bed load transport is large. Therefore, no sedimentation but erosion takes place in this reach with these calculations. There are three alternative explanations for this conflicting result: 1) The calculations are not accurate enough, because of too many simplifications: use of an average slope, simplified hydraulic geometry, a fixed roughness length and grain-size. 2) There is actual deposition, because the sediment input exceeds the predicted sediment transport capacity. 3) There is actual erosion in the steep reach. It is possible that different periods of sediment overloading have caused the river to anastomose, while in the present situation erosion takes place, to create a more stable situation with a lower gradient. From the genetic profiles, it becomes clear that there is indeed sedimentation in this area in a time frame of 3000 years. However, this is no evidence that sediment deposition took place during the whole period. So net accumulation can take place on a time scale of thousands of years, but sediment transport can vary over the years due to differences in sediment input, hydraulics and morphology, causing periods with erosion.

This idea of an irregular sedimentation process driving the river to anastomose is confirmed by analyzing the channel chronology of the catchment (Section 4.5). To have an anastomosing system, multiple channels systems have to be active at the same time. This is regulated by the equilibrium between formation of new channels and slow abandonment of older channels (Section 2.4). Figure 19 however, displays that this process is not a continuous process. This figure suggests different periods wherein channels become abandoned and new channels are formed. This does not support the theory of a constant overload of sediment causing the system to anastomose, but can point to different periods of sediment overloading causing the river to anastomose. During these periods with sediment overloading, channel instability occurs. In this theory, net erosion can take place in the present situation, whereas accumulation takes places in a period with excessive sediment supply.

De Haas (2010) analyzed the bed evolution of the upper Columbia River, to establish whether the bed configuration of the modeled upper Columbia River reach is an equilibrium bed configuration. The present-day bed configuration is characterized by the transition of the slope from gentle to steep and back to gentle as described by Abbado et al. (2005).

In the model of De Haas (2010), a situation with a sediment supply equal to the transport capacity gives a bed that rapidly adjusts its slope until an equilibrium slope is reached comparable to the measured slope of the gentle reach upstream of Spillimacheen and between Castledale and Golden. Consequently, it can be concluded that the gentle reach of the current upper Columbia River is the equilibrium slope, whilst the presence of the steep slope is not an equilibrium situation. To obtain the present-day bed

configuration of the modeled reach, De Haas (2010) added a sediment pulse to the model, whereby the slope increases, which causes the sediment transport capacity to increase. Consequently, more sediment is transported along this newly formed steep reach. This sediment is then deposited at the downstream end of this steep reach. So, as time passes, the steep reach expands itself until finally in the entire modeled reach a steeper bed slope has formed. At the moment the sediment pulse stops, the new steep slope is steeper than the original equilibrium slope. Therefore the transport capacity is larger than the upstream sediment feed; this causes erosion. Initially, the bed in the upstream part of the steep reach is eroded and the bed slope in this part of the reach adjusts itself to the new upstream sediment feed. Consequently, the transport capacity in this part of the reach becomes in equilibrium with the sediment transport. Now, the erosion mainly occurs more downstream, where the slope is still steep. This process continues until finally the bed is in equilibrium with the upstream sediment feed.

So, the presumed irregular sedimentation process from the sediment transport predictors and the channel chronology is confirmed by the modeled bed evolution of De Haas (2010). To obtain a reach with differences in slope, a sediment pulse is needed. It is likely that a period of sediment overloading causes an increase in channel activity, and thus an increase in the degree of anastomosis.

5.4 Origin of anastomosis

The aim of the research is to explore the origin of anastomosis. One existing hypothesis about the origin of anastomosis is tested during this research. This hypothesis of Abbado et al. (2005) and Makaske et al. (2009) suggest an upstream control. But, as presented in Chapter 2, three other hypotheses about the origin of anastomosis exist, these will be discussed here. After that the research questions will be addressed, to see if the hypothesis of upstream control holds.

Hypothesis 1: Deltaic origin of anastomosis

A hypothesis about the origin of the anastomosing upper Columbia River is that the river is at a final stage, formed after the deltaic infilling of lakes in the valley, with channel splitting around mouth bars. The geomorphology of the valley forces the river to confluences, whereby it is not possible for the river to expand like a delta. But the Laitaure delta has also converging channels, so this does not reject this hypothesis. The largest difference between a delta and the upper Columbia River is the absence of deltaic mouth bars and the ending of the river in a single channel instead of multiple channels. Analysis of borehole cross-sections also does not show evidence for a deltaic lake fill with mouth bars. Also large scale lacustrine deposits are missing. So no evidence for the deltaic origin of anastomosis is found, which makes this hypothesis not plausible.

Hypothesis 2: Downstream control

Smith (1983) proposed that the cause of frequent avulsions is the rise in base level (downstream control).

But in central Australia, anastomosing rivers exist under a relatively stable base level (Makaske, 2001, after Rust, 1981; Nanson et al., 1986; Gibling et al., 1998). And the alluvial fans in the upper Columbia River are presently not active, and therefore base level is presently stable. Also, no significant change in slope is measured in the Columbia Valley near an alluvial fan. This makes it unlikely that these fans influence the present river system. Although, when the river system has a large response time, the present river pattern can be determined by former active alluvial fans. This response time is not known from this research. Also, the backwater adaptation length of the river is not calculated during this research. So, this hypothesis is not rejected nor confirmed here.

Hypothesis 3: Optimizing sediment transport

Huang and Nanson (2000, 2007) proposed that anastomosing rivers are adjusted in geometry and hydraulic friction to optimize transport of water and sediment discharges. Not all rivers show this efficiency of transporting water and sediment by multiple channels. In the case of the upper Columbia River, the bulk of the water and sediment moves through a single channel (Makaske, 2001). Even at high flow, the secondary channels have only a modest function for discharging the water. Makaske (1998) and Abbado et al. (2005) demonstrated that these secondary channels are less efficient in transporting sediment. Bed load transport of the upper Columbia River strongly decreases downstream. Therefore, this multiple channel system can not be taken as a response of the system to maximize water and sediment throughput. Tabata and Hickin (2003) did also not support the hypothesis of enhancing water and sediment discharge. Based on their observations on the upper Columbia River; they found that channel splitting leads to hydraulic inefficiency. Possibly, two types of anabranching exist: one efficient and the other less so (Jansen and Nanson, 2004). Although more anastomosing rivers, including the upper Columbia River, must be investigated to get better data of bed load transport capacity to totally invalidate this hypothesis.

From this discussion of the hypotheses it becomes clear that hypotheses 1 and 3 are not likely. Hypothesis 1 (deltaic origin of anastomosis) is rejected because no lacustrine and deltaic morphology characteristics are found. Hypothesis 3 (optimizing sediment transport) was already rejected by previous researches to the upper Columbia River. Hypothesis 2 (downstream control) is not confirmed nor rejected; it is possible that this hypothesis is true when the response time to a rise in base level of the river system is large. The hypotheses of Abbado et al. (2005) and Makaske et al. (2009) (upstream control) is the most likely explanation of the origin of anastomosis in this study as is shown by the geological reconstruction of the floodplain sediments in the upper Columbia River valley. During this research, it was found that bed-material load deposition is higher in the upper (highly) anastomosing reach than in the lower (less) anastomosing reach. This supports the hypothesis of upstream control as reason for the origin of the anastomosing upper Columbia River.

5.4.1 Research questions

Is anastomosis a disequilibrium feature resulting from an overload of sediment on a low-energetic system?
Yes. The results of Makaske et al. (2009) are confirmed by the results derived after sediment budget calculations made by analysing floodplain-wide transects in the upper and the lower anastomosing reach. The deposits in the upper anastomosing reach consist of more bed-material load than in the lower anastomosing reach. Sedimentation rates derived from these cross-sections show a higher long-term average sedimentation rate in the upper anastomosing reach than in the lower anastomosing reach. This is proved by AMS radiocarbon dates, used to calculate the long-term average sedimentation rate. However, bed load transport predictions based on the present-day river characteristics indicate erosion in the upper anastomosing reach and deposition in the lower anastomosing reach. This can be the result of inaccuracy of the bed load transport predictions, or of a change in the situation of sediment overloading, whereby sediment overloading takes places in pulses.

Is the network of multiple channels of the upper Columbia River stable and is it an equilibrium feature?
No. The positions of the channel bodies in the three cross-sections suggest that there are periods with more and with less channel activity. The plotted depths of the levees bases are clustered, indicating periods with more and less channels. This picture is most clear in the upper anastomosing reach. The lower anastomosing reach seems more stable. This idea is confirmed by the bed load transport predictions, which indicates a present situation with erosion in the upper anastomosing reach, which also points to a system driven by phases of sediment overloading. The anastomosis of the upper Columbia River is generated from the inability of the river to transport its entire sediment load, leading to in-channel aggradation and avulsions. Furthermore, the upper Columbia River channels have no ability to migrate laterally, because of low stream power and erosion-resistant banks. This is caused by the intrinsic factors as low floodplain gradient and cohesive bank material. Because of the lateral channel stability, no lateral storage capacity for the surplus of sediment load is created. Therefore, much of the bed-material load is stored on the channel bed, leading to gradual decrease in flow capacity, increased overbank flooding and sedimentation, crevassing and cutting of new channels on the floodplain. So, the upper Columbia River is in a dynamic equilibrium of frequent avulsions and slow abandonment of older channels.

6 Conclusions

The aim of this research was to determine the origin of anastomosis by testing if excessive sediment supply is the driving mechanism of anastomosis. The following conclusions can be made after this research:

- Anastomosis is a disequilibrium feature resulting from an overload of sediment. The deposits in the upper (highly) anastomosing reach consist of more bed-material load than in the lower (less) anastomosing reach. And the sedimentation rates derived from the cross-sections and the AMS radiocarbon dates show a higher long-term average sedimentation rate in the highly anastomosing reach than in the weakly anastomosing reach.
- The network of multiple channels of the upper Columbia River is not stable. The positions of the channel sand bodies and levee bases in the three cross-sections suggests that there are periods with more and with less channel activity, probably caused by periods with more and less sediment overloading.
- The anastomosing character of the upper Columbia River can be explained by an intrinsic response to local factors (low floodplain gradient, restricted floodplain width) and a response to allogenic factors (excessive sediment supply pulses).
- The anastomosis of the upper Columbia River is generated from the inability of the river to transport its entire sediment load, leading to in-channel aggradation and avulsions and the river have no ability to migrate laterally, because of low stream power and erosion-resistant banks.

So, the upper Columbia River is in a dynamic equilibrium of frequent avulsions and slow abandonment of older channels driven by periods of sediment overloading. This confirms and expands the hypothesis of Abbado et al. (2005) and Makaske et al. (2009).

References

Abbado, D., Slingerland, R., Smith, N.D. (2005). Origin of anastomosis in the upper Columbia River, British Columbia, Canada. In: Blum, M.D., Marriot, S.B., Lelair, S.M. (Eds.), *Fluvial Sedimentology VII. Special Publucationof the International Association of Sedimentologists 35,* Blackwell Oxford, UK, 3-15.

Andrén, H. (1994). Development of the Laitaure Delta, Swedish Lappland. A study of growth, distributary forms and processes. Institute of Earth Sciences, Physical Geography, Uppsala University. UNGI Rapport 88, 188 pp.

Axelsson, V. (1967). The Laitaure delta, a study of deltaic morphology and processes. *Geografiska Annaler 49A: 1*, 127 pp.

Berendsen, H.J.A. and Stouthamer, E. (2001). Palaeogeographic Development of the Rhine-Meuse Delta, the Netherlands. Van Gorcum, Assen, 268 pp.

De Haas, T. (2010). Network dynamics and origin of anastomosis, upper Columbia River, British Columbia, Canada. MSc Thesis, Faculty of Geosciences, Utrecht University, Utrecht.

Erkens, G. (2009). Sediment dynamics in the Rhine catchment, quantification of fluvial response to climate change and human impact. Nederlandse Geografische Studies vol. 388. Koninklijk Nederlands Aardrijkskundig Genootschap/ Faculteit Geowetenschappen, Universiteit Utrecht, Utrecht.

Frings, R.M. (2007). Downstream fining in large sand-bed rivers. *Earth-Science Reviews 87*, 39-60.

Frings, R.M., Kleinhans, M.G., Vollmer, S. (2008). Discriminating between pore-filling load and bed-structure load: a new porosity-based method, exemplified for the river Rhine. *Sedimentology 55,* 1571-1593.

Google Earth, version 5.0.11733.9347, May 5th 2009.

Halley, P, photographer, www.patricehalley.com, website visited in 2010.

Huang, H.Q. and Nanson, G.C. (2000). Hydraulic geometry and maximum flow efficiency as products of the principle of least action. *Earth Surface Processes and Landforms 25*, 1-16.

Huang, H.Q. and Nanson, G.C. (2007). Why some alluvial rivers develop an anabranching pattern. *Water resource research 43*, 1-12.

Jansen, J.D. and Nanson G.C. (2004). Anabranching and maximum flow efficiency in Magela Creek, northern Australia. *Water Resources Research 40*, 1-12.

Jerolmack, D.J. and Mohrig, D. (2007). Conditions for branching in depositional rivers. *The Geological Society of America 35*, 463-466.

Kleinhans, M.G., Jagers, H.R.A., Mosselman, E., Sloff, C.J. (2008). Bifurcation dynamics and avulsion duration in meandering rivers by one-dimensional and three-dimensional models. *Water resources research 44*, 1-31.

Lauer, J.W. and Parker, G. (2008). Net local removal of floodplain sediment by river meander migration. *Geomorphology 96*, 123–149.

Locking, T. (1983). Hydrology and sediment transport in an anastomoing reach of the upper Columbia River, B.C. MSc thesis, Department of Geography, University of Calgary, Alberta, Canada.

LLG 2008 borehole data program, version 1.3.6.0 (2008). Vollenberg, K.P., Department of physical geography, Utrecht University, Utrecht.

Makaske, B. (1998). Anastomosing rivers: forms, processes and sediments. Nederlandse Geografische Studies vol. 249. Koninklijk Nederlands Aardrijkskundig Genootschap/ Faculteit Ruimtelijke Wetenschappen, Universiteit Utrecht, Utrecht.

Makaske, B. (2001). Anastomosing rivers: a review of their classification, orgin and sedimentary products. *Earth-Science Reviews 53*, 149-196.

Makaske, B., Smith, D.G., Berendsen, H.J.A. (2002). Avulsions, channel evolution and floodplain sedimentation rates of the anastomosing upper Columbia River, British Columbia, Canada. *Sedimentology 49,* 1049-1071.

Makaske, B., Smith, D.G., Berendsen, H.J.A., de Boer, A.G., van Nielen-Kiezebrink, M.F., Locking, T. (2009). Hydraulic ans sedimentary processes causing anastomosing morphology of the upper Columbia River, Britisch Columbia, Canada. *Geomorphology 111,* 194-205.

Nanson, G.C. and Knighton, D. (1996). Anabranching rivers: Their cause, character and classification. *Earth surface processes and landforms 21,* 217-139.

Schumm, S.A. (1985). Patterns of alluvial rivers. *Annual Review of Earth and Planetary Sciences 13,* 5–27.

Smith, D.G. (1983). Anastomosed fluvial deposits: modern examples from Western Canada. In: Collinson, J. and Lewin, J. (Eds.), *Modern and Ancient Fluvial Systems. Special Publication of the International Association of Sedimentologists 6*. Blackwell, Oxford, 155-168.

Smith, N.D., Cross, T.A., Dufficy, J.P., Clough, S.R. (1989). Anatomy of an avulsion. *Sedimentology 36*, 1–23.

Stouthamer, E. (2001). Sedimentary products of avulsions of the Holocene Rhine-Meuse Delta, The Netherlands. *Sedimentary Geology 145*, 73-92.

Tabata, K.K. and Hickin, E.J. (2003). Interchannel hydraulic geometry and hydraulic efficiency of the anastomosing Columbia River, Southeastern British Columbia, Canada. *Earth Surface Processes and Landforms 28*, 837-852.

Ten Brinke, W.B.M., Bolwidt, L.J., Snippen, E., Van Hal, L.W.J. (2001). Sedimentbalans Rijntakken 2000. Een actualisatie van de sedimentbalans voor slib, zand en grind van de Rijntakken in het beheersgebied van de Directie Oost-Nederland. Rijksinstituut voor Integraal Zoetwaterbeheer en Afvalwaterbehandeling/RIZA, rapport 2001.043.

Törnqvist, T.E., De Jong, A.F.M., Oosterbaan, W.A., Van der Borg, K. (1992). Accurate dating of organic deposits by AMS ^{14}C measurement of macrofossils. *Radiocarbon 34*, 566–577.

Van den Berg, J.H. (1995). Prediction of alluvial channel pattern of perennial rivers, *Geomorphology 12,* 259-279.

Van der Plicht, J. (1993). The Groningen radiocarbon callibration program. *Radiocarbon 35,* 231.237.

Van Rijn, L.C. (1984). Sediment transport, part I. Bed load transport. *Journal of hydraulic engineering 110*, 1431-1456.

Whetten, J.T., Kelley, J.C., Hanson, L.G. (1969). Characteristics of Columbia River sediment and sediment transport. *Journal of Sedimentary Petrology 39*, 1149-1166.

Appendix

Ask me for the files: evalavooi@gmail.com. Images shown here are previews.

Appendix 1 Core descriptions

Appendix 2 Borehole location in transect Harrogate

Appendix 3 Borehole location in transect Parson

Appendix 4 Borehole cross-sections

Appendix 5 Genetic interpretation of the borehole cross-sections – version 1

Appendix 6 Genetic interpretation of the borehole cross-sections – version 2

Appendix 2 - Borehole location in transect Harrogate

Appendix 3 - Borehole location in transect Parson

Appendix 4 - Lithological borehole cross-sections

A Harrogate

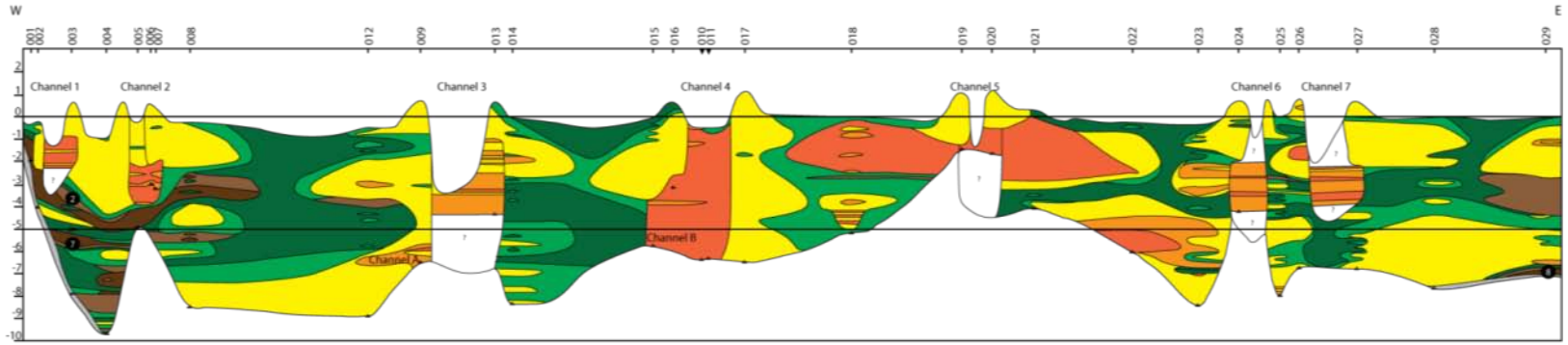

B Castledale

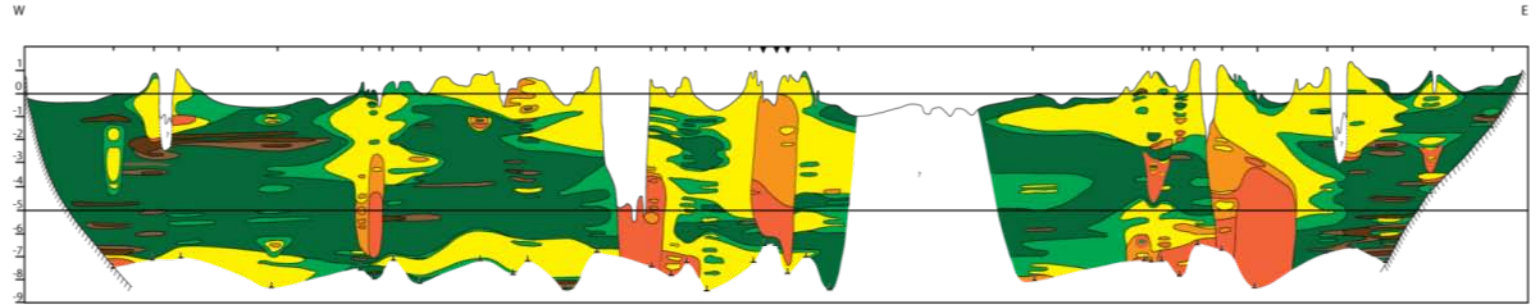

C Parson

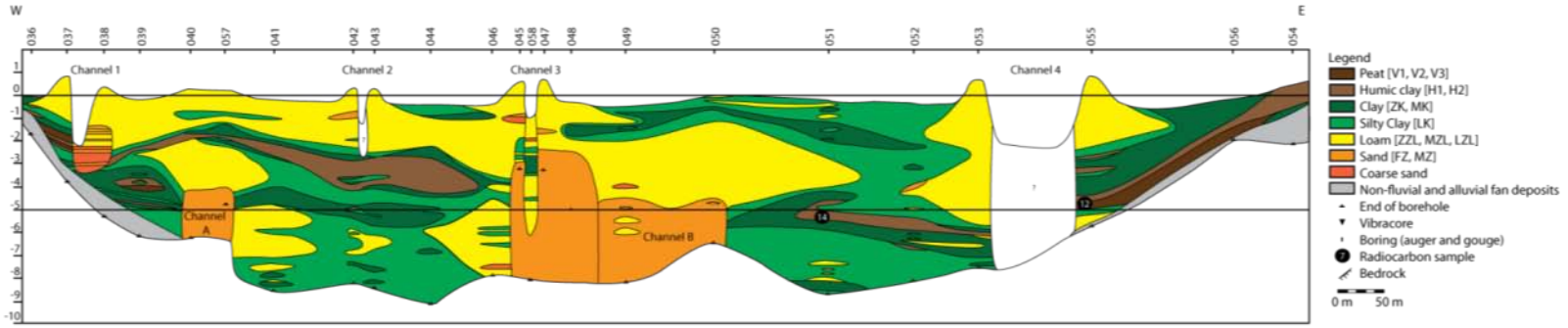

Appendix 5 - Genetic interpretation of the borehole cross-sections - version 1

A Harrogate

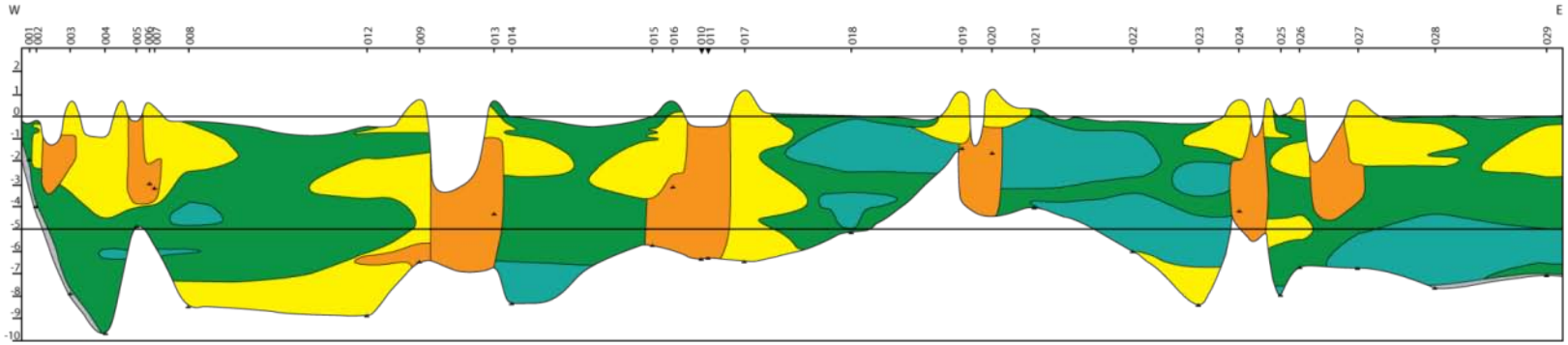

B Castledale

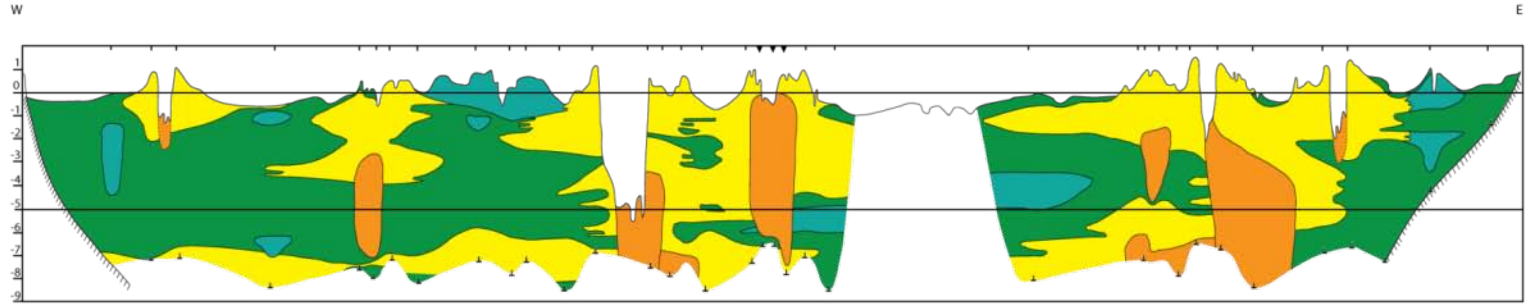

C Parson

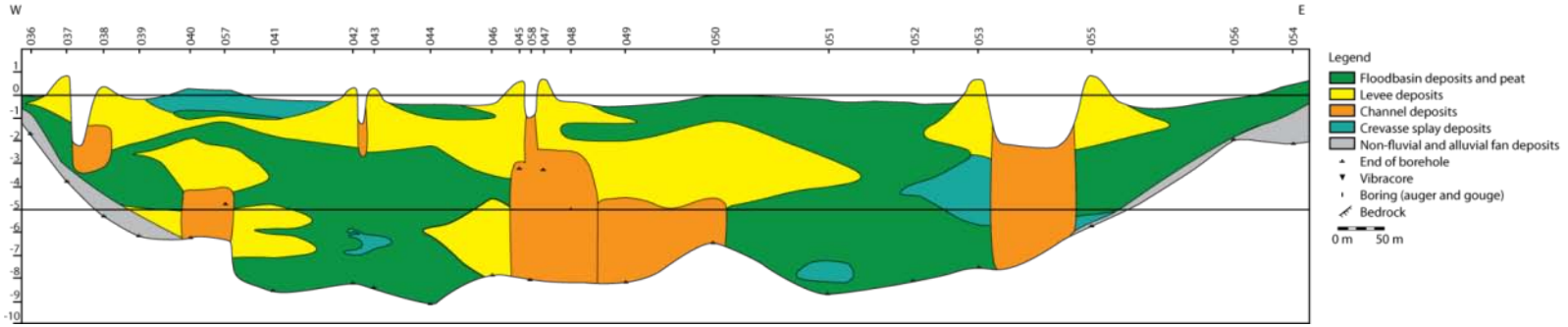

Appendix 6 - Genetic interpretation of the borehole cross-sections - version 2

A Harrogate

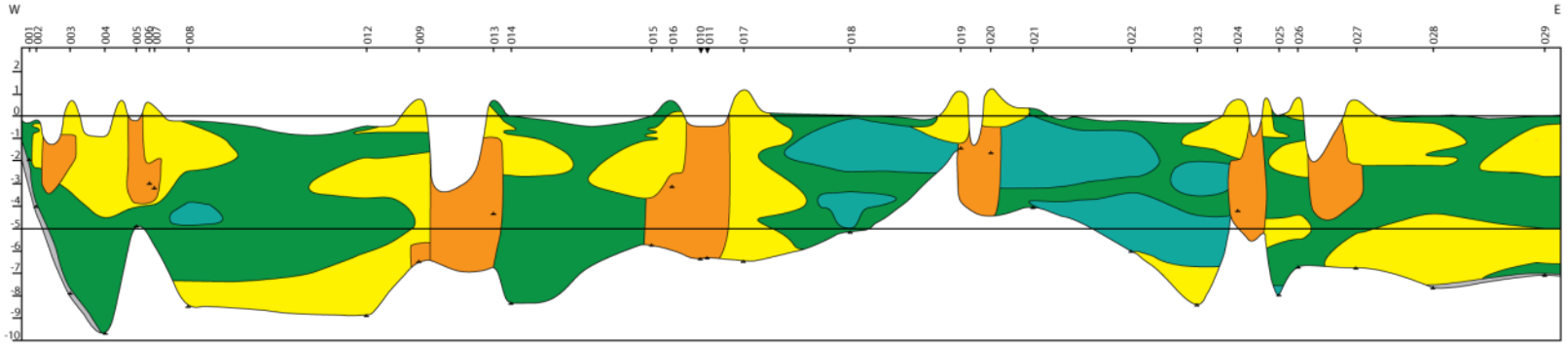

B Castledale

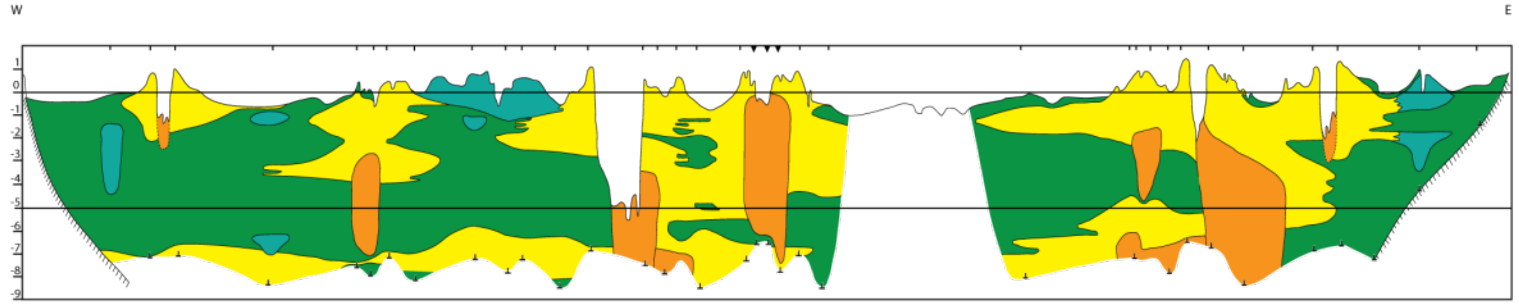

C Parson